journal

Mechanism for Salt Scaling

John J. Valenza II[†] and George W. Scherer

Princeton Institute for the Science & Technology of Materials, Department of Civil and Environmental Engineering,
Princeton, New Jersey 08540

Over the past 60 years, concrete infrastructure in cold climates has deteriorated by "salt scaling," which is superficial damage that occurs during freezing in the presence of saline water. It reduces mechanical integrity and necessitates expensive repair or replacement. The phenomenon can be demonstrated by pooling a solution on a block of concrete and subjecting it to freeze/thaw cycles. The most remarkable feature of salt scaling is that the damage is absent if the pool contains pure water, it becomes serious at concentrations of a few weight percent, and then stops at concentrations above about 6 wt%. In spite of a wealth of research, the mechanism responsible for this damage has only recently been identified. In this article, we show that salt scaling is a consequence of the fracture behavior of ice. The stress arises from thermal expansion mismatch between ice and concrete, which puts the ice in tension as the temperature drops. Considering the mechanical and viscoelastic properties of ice, it is shown that this mismatch will not cause pure ice to crack, but moderately concentrated solutions are expected to crack. Cracks in the brine ice penetrate into the substrate, resulting in superficial damage. At high concentrations, the ice does not form a rigid enough structure to result in significant stress, so no damage occurs. The morphology of cracking is predicted by fracture mechanics.

I. Introduction

CONCRETE (see sidebar 1, Cement and Concrete) is the most widely used material in the world. The raw materials are ubiquitous, so it is relatively inexpensive, but concrete poses numerous durability issues that result in high maintenance costs. The National Research Council estimates that repair of the infrastructure in the United States costs nearly $50 billion annually.[1] Moreover, the cost of new roadways, bridges, and terminals is estimated at hundreds of billions of dollars annually. Clearly, improving the durability of concrete has huge social and economic implications.

Salt scaling is defined as superficial damage caused by freezing a saline solution on the surface of a cementitious body. The damage is progressive and consists of the removal of small chips or flakes of material. These characteristics were first revealed in the

1950s through laboratory testing,[2,3] and they were subsequently verified through field tests.[4] In moderate to extreme cases, this damage culminates in exposure of the coarse aggregate (Fig. 1).

In cold climates, salts are regularly used to de-ice roadways and walkways. Consequently, salt scaling is one of the major durability issues facing cementitious materials in this climate. While salt scaling alone will not render a structure useless, it results in accelerated ingress of aggressive species, such as chlorides, and the propensity for a high degree of saturation. The former renders the body susceptible to corrosion of the reinforcing steel,[5–7] while the latter results in strength loss from internal frost action[8–10] (Fig. 1). Both of these effects diminish the service life of concrete.

Hundreds of laboratory and field studies have clearly identified the characteristics of salt scaling, but have not explained the cause. The most well-known characteristic is that a maximum amount of damage is achieved with a moderate amount of salt. This "pessimum" concentration is widely accepted to be at a solute concentration of ~3% by weight, independent of the solute used[2,3,11–15] (Fig. 2). A number of mechanisms have been proposed to explain various features of salt scaling, but none has been able to account for all of the observed characteristics, until recently.[16,17] In the next section, we will summarize the features of salt scaling, and then offer a new explanation that accounts for all of them.

II. Phenomenology

Figure 2 shows the results of a classic study of salt scaling that demonstrated the existence of a pessimum concentration of solute. Blocks of concrete were covered with a pool of water containing various concentrations of solute, and then exposed to freeze/thaw cycles. The most striking result was that the damage was the worst at intermediate concentrations of solute, regardless of the type of solute (inorganic salt, alcohol, urea). This study also showed that damage did not occur if the solution was poured off the sample before freezing. After other studies confirmed that the pessimum concentration was around 3 wt%, standard tests of resistance to scaling were developed using 3% solutions of NaCl.

One standard method is the American Society for Testing and Materials (ASTM) standard C672.[18] A solution 6 mm deep is confined on the surface of a sample ≥ 75 thick, which is cooled to $-17.8° \pm 2.8°C$ in 16–18 h, and then thawed at $23° \pm 3°C$ for 6–8 h. The amount of damage is quantified visually (rated on a scale of 0–5, 0 = no scaling, 5 = severe scaling), and by change in

Feature

Sidebar 1. Cement and Concrete

Portland cement is made by firing a combination of limestone and clay, with minor additions of other components to influence the liquidus temperature and phase development during cooling. After reacting at $\sim 1500°C$, the products are a mixture of calcium silicate and aluminum silicate phases that are reactive with water. This material is ground to an average particle size around 30 μm, which is known as cement. The product obtained by mixing cement with water is cement paste; mortar is a composite of sand (grains <5 mm) with paste, and concrete contains both sand and coarser aggregate. The most important contributors to strength development in cement paste are tricalcium silicate ($3CaO \cdot SiO_2$, called alite) and slightly less reactive dicalcium silicate ($2CaO \cdot SiO_2$, called belite). [The most reactive mineral in Portland cement is tricalcium aluminate, which would cause premature setting (making it virtually impossible to cast concrete into molds). This problem is avoided by adding gypsum to the cement, which reacts with the aluminate to form needles of ettringite that do not cause stiffening of the paste.] When water reacts with alite and belite, the product is calcium–silicate–hydrate (C–S–H), which is a gelatinous substance with no fixed stoichiometry, but with an average composition close to $1.7CaO \cdot SiO_2 \cdot 4H_2O$. After cement and water are mixed, C–S–H begins to form in the water, and binds the structure together as it deposits on the surfaces of the cement particles. If the water/cement ratio (by weight) is below about 0.4, then the volume of C–S–H is sufficient to fill completely the space originally occupied by water; even at $w/c \sim 0.6$, the C–S–H can depercolate the channels originally containing water. When this happens, the permeability of the paste is very low, because the pores in the C–S–H are in the nanometer range. In mortar or concrete, the cement particles do not pack as densely against the aggregate particles as they do in pure paste, so there is a region of enhanced porosity at the paste/aggregate interface called the interfacial transition zone (ITZ). Its width is roughly equal to the size of a cement grain (20–50 μm). The ITZ profoundly affects the strength of concrete, because cracks first form and spread along the interface, and it dominates the permeability. The larger pores in the ITZ may result in preferential formation of ice, but this has not been demonstrated. To protect against frost damage, chemical additives called air entrainment agents (AEA) are added to the water during mixing of concrete. The AEA are surfactants that encourage formation of air bubbles ~ 50–150 μm in diameter. Their function is discussed in the sidebar on Internal Frost. In addition to these air voids, there is typically ~ 3 vol% air that is mechanically entrapped in concrete during mechanical mixing of the ingredients.

mass. European standards use similar temperature cycles, but judge the damage quantitatively by weighing the debris after various numbers of cycles.[19,20] Most of the studies cited here use variants of the latter procedure.

Numerous studies have revealed the following characteristics of salt scaling (representative citations noted):

1. Salt scaling consists of the progressive removal of small flakes or chips of binder.[2,21,22]

2. A pessimum exists at a solute concentration of $\sim 3\%$, independent of the solute used.[2,3]

3. No scaling occurs when the pool of solution is missing from the concrete surface.[3,12,14]

4. No damage occurs when the minimum temperature is held above $-10°C$[12,23]; the amount of damage increases as the minimum temperature decreases below $-10°C$[11,12,14,24] and with longer time at the minimum temperature.[12,25]

5. Air entrainment improves salt scaling resistance.[12,23,26–29]

6. The salt concentration of the pool on the surface is more important than the salt concentration in the pore solution.[13,15]

7. Susceptibility to salt scaling is not correlated with susceptibility to internal frost action.[13,29–31]

8. The strength of the surface governs the ability of a cementitious body to resist salt scaling.[17]

Previous explanations for the cause of salt scaling invoke pore chemistry (see sidebar 2, Role of Salt) or attribute the damage to the same causes as internal frost action (see sidebar 3, Internal Frost Action). However, neither of these explanations adequately accounts for all of the characteristics listed above.[16] In the remainder of this article, we explain how the glue-spall mechanism produces all of the features of salt scaling. In the next section, we describe the glue-spall mechanism. In Section *IV*, we discuss the mechanical and viscoelastic properties of brine ice. In Section *V,* we present the results of a viscoelastic stress calculation that shows why the pessimum occurs at 3% solute. The fracture mechanics of salt scaling, discussed in Section *VI*, accounts for both the depth and morphology of this damage. In Sections *VII* and *VIII,* we present experimental evidence showing that the glue-spall mechanism is active when a saline solution
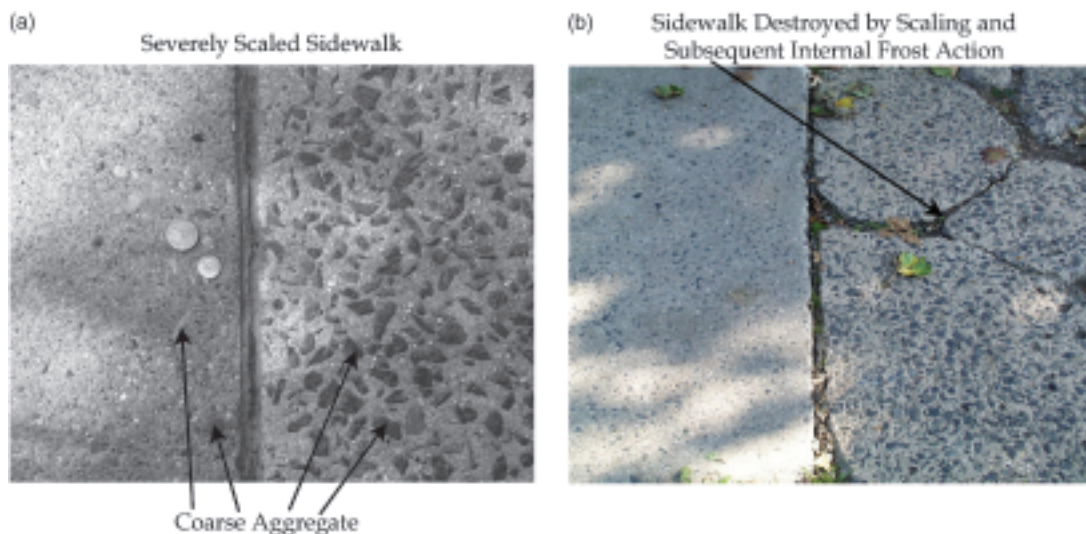

Fig. 1.　(a) Picture of a severely scaled sidewalk. (b) Sidewalk that was severely scaled, which led to a complete loss of mechanical integrity, probably by internal frost damage.
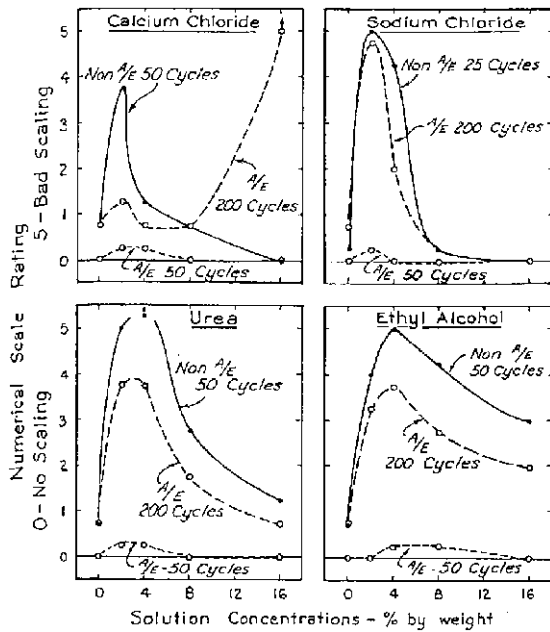
Fig. 2. Results from Verbeck and Klieger[3] (Figure 2, p. 3) indicate that a maximum amount of damage occurs at a solute concentration of ∼3%, and that this trend is independent of the solute (sodium chloride, calcium chloride, urea or ethyl alcohol). These results also illustrate the beneficial effect of air entrainment (A/E).

is frozen on a cementitious surface. The results are summarized in Section IX.

III.　Glue-Spall Mechanism

Glue-spalling is a technique used to decorate a glass surface.[46] The procedure consists of spreading epoxy on a sandblasted glass surface, allowing the epoxy to cure, and then lowering the temperature of the composite (Fig. 4(b)). During cooling, the stress from the thermal expansion mismatch causes the epoxy to crack into small islands. High tensile stresses are created in the glass surface at the boundary of the islands as the epoxy shrinks relative to the substrate (Fig. 4(e)—σ_{gs}). These stresses propagate cracks in the glass surface, culminating in the removal of the island and a thin piece of glass (Fig. 4(c)).

In 1982, Gulati and Hagy analyzed the stresses in an epoxy/glass composite exposed to a uniform temperature change and performed a finite element calculation that confirmed their analytical solution.[47] The elastic analysis approximates the glue-spall stress in the glass surface as the difference between the stress from the thermal expansion mismatch and the tensile stress in the epoxy:

$$\sigma_{gs} = \left(\frac{E_g}{1-\nu_g}\right)\left[\Delta\alpha\Delta T - \sigma_e\left(\frac{1-\nu_e}{E_e}\right)\right] \qquad (3)$$

where σ is the stress parallel to the x-axis (Fig. 4(d)), E is the elastic modulus, ν is Poisson's ratio, $\Delta\alpha = \alpha_e - \alpha_g$ is the thermal

---

Sidebar 2.　Role of Salt

Several mechanisms have been suggested by which salt might contribute to scaling damage: (1) precipitation of salt creating crystallization pressure; (2) chilling from sudden melting of ice when salt is applied; and (3) osmotic pressure. However, we will show that none of these may be responsible for salt scaling. Crystallization of salt can certainly cause destructive stresses.[32] However, NaCl does not precipitate from a brine until the temperature drops below the eutectic at −22°C. As that temperature is not reached in conventional scaling tests, and rarely occurs outdoors in most locations, growth of salt crystals is not the culprit in salt scaling. Salt strongly reduces the melting point of ice, as shown in Fig. 5(a), so deicer salts are applied in sufficient quantity to lower the melting point below ambient temperature. The heat necessary to cause this melting is withdrawn from the surface of the concrete body, so a temperature gradient forms in the surface, resulting in differential strain and stress.[33] However, field measurements indicate that the temperature shock experienced when salt is spread on the ice layer[33] is not large enough to result in damaging stresses.[34] Moreover, this mechanism is not consistent with the procedure used in the standard test method,[18–20] which consists of freezing a saline solution on the surface of a concrete slab. The pore liquid in cement naturally contains dissolved ions in concentrations around 0.5M, and the concentration may be higher after the pore liquid equilibrates with the external solution (see sidebar 4, Salt Swelling). When ice forms in the pores, the solute is not incorporated into the ice, so the liquid adjacent to the ice is enriched in solute relative to the bulk of the solution. Consequently, there is a tendency for water to diffuse toward the zone of high concentration (i.e., toward the ice/water interface), causing the fluid pressure to rise. In principle, this effect could raise the pressure to the osmotic pressure, Π, which is the pressure necessary to prevent the diffusion of water molecules.[35] In the present case, the osmotic pressure results from the difference in mole fraction of solvent, x, between the ice/solution interface (x_0) and that of the pore liquid far from the ice (x_∞), which is

$$\Delta\Pi = \Pi(x_0) - \Pi(x_\infty) = -\frac{RT}{\bar{V}_L}\ln\left(\frac{x_0}{x_\infty}\right) \qquad (1)$$

where R is the ideal gas constant and $\bar{V}_L$ is the partial molar volume of water. As a result of the osmotic pressure, a tensile hoop stress will arise in the pore wall, where $\sigma_\theta \approx \Delta\Pi/2$. The potential for this stress to rise above the concrete tensile strength occurs when the salt concentration differs by ∼14%; if x_0 is equal to the liquidus composition (which is the highest value it could reach), then Eq. (1) predicts damaging tensile stress at temperatures below about −10°C.[34] In fact, the osmotic pressure will never evolve to a damaging level, because the rising pressure is quickly relieved by fluid flow. If diffusion raises the pressure near the ice, then Darcy flow will relax the pressure, and flow is faster than diffusion. The characteristic time for hydrodynamic relaxation of a pressure gradient is proportional to the square of the distance over which the gradient exists, $\tau_R \propto L^2$.[36] Our experiments yield $\tau_R \approx 700$ s for a plate of cement paste ($w/c = 0.45$) with a half-thickness of 1.5 mm.[37] Assuming that the concentration gradient occurs over a distance of 400 μm (typical of the largest air void spacing in concrete), the pressure will be relieved by fluid flow in 700 (0.4/1.5)^2 = 50 s. Given $D \approx 1.3 \times 10^{-7}$ cm^2/s[34] (see sidebar 4, Salt Swelling), the time required to build up the osmotic pressure is $t \approx x^2/D \approx (0.04$ cm$)^2/(1.3 \times 10^{-7}) \approx 1.2 \times 10^4$ s in the same paste. Even if the concentration gradient were 100 times narrower than the spacing between air voids, the time to build up the osmotic pressure would be much longer than that required to relieve the pressure by flow. Therefore, hydrodynamic relaxation prevents the formation of destructive osmotic pressure.

Sidebar 3.   Internal Frost Action

It is widely believed that frost damage results from the 9% increase in volume as water transforms to ice. However, the damage from freezing of concrete is actually a result of crystallization pressure.[10,16,34] The stress exerted on porous bodies by crystals of salt or ice follows from the fact that the solids repel one another. That is, there is a film of liquid (of unknown thickness, but estimated to be less than 1 nm) separating the surfaces of the growing crystal and the pore wall. Contact between the two crystals would create an interface with high energy, so the energy of the system is lower if both solids are in contact with liquid. In the case of ice, the van der Waals forces alone provide a large enough repulsive force so that stresses exceeding the tensile strength of concrete would be required to push ice into contact with the mineral surface.[9] To avoid destructive pressure from growth of ice in the pores, air voids are deliberately introduced into concrete. It was originally thought that these voids provided sinks for the water displaced by the volume change,[38] but it was subsequently realized that the voids serve as nucleation sites for ice,[39] as explained below. When ice forms in a pore, the ice occupies more volume than the water from which it formed. As the adjacent water is pushed away, pressure builds up to a degree that depends on the rate of growth of the crystal, the permeability of the pore system (which controls the resistance to movement of the water), and the distance to the nearest free surface. Powers[38] modeled this phenomenon and demonstrated that the pressure could be kept at a safe level if closely spaced air voids were introduced into concrete to serve as sinks for the displaced water. His calculation was conservative in several respects. First, as he noted, the pressure will only develop if the saturation exceeds 91% in the pores near the ice. Second, the pressure depends on the rate of growth, which will be controlled by heat flow, and is therefore likely to be relatively slow. Powers and Helmuth[39] later concluded that hydraulic pressure was unimportant, and that the real role of the air voids was to provide nucleation sites where ice could grow without constraint.As explained below, crystals in the voids suck liquid from the small pores of the paste and thereby impose compressive stresses on the concrete. If a crystal has a radius of curvature r, then its melting point (T_m) is lower than that of an infinitely large crystal by an amount given by the Gibbs–Thomson equation[9]:

$$T_m(\kappa_{CL}) = T_m(0) - \frac{\gamma_{CL}\kappa_{CL}}{\Delta S_{fv}} \qquad (2)$$

where γ_{CL} is the crystal/liquid interfacial energy, ΔS_{fv} is the entropy of fusion per unit volume of crystal, and $\kappa_{CL} = 2/r$ is the curvature of the crystal/liquid interface. For a crystal to exist in a small pore, as in Fig. 3(b), the temperature must be lower than $T_m(\kappa_{CL})$, where $\kappa_{CL} = 2/(r_p-\delta)$ and δ is the thickness of the unfrozen water layer. When the temperature is reduced below $T_m(2/(r_p-\delta))$, the crystal will bulge into the mouths of intersecting pores (radius $r_E<r_P$) until the curvature satisfies Eq. (2). To preserve equilibrium in the crystal, the pore wall imposes a confining pressure on the surfaces of the crystal (Fig. 3(b)—red arrows), which results in tensile hoop stress in the pore wall. The magnitude of the confining pressure is proportional to the difference in curvature between the surface of the crystal bulging into the intersecting pore and that adjacent to the pore wall.[10] Therefore, the pressure is maximized when the pore confining the crystal is much larger than the intersecting pores. It is this stress that results in microcracking and weakening of concrete during internal freezing. When crystals form in an air void (10–1000 μm in diameter), which are several orders of magnitude larger than the inherent porosity of cement paste ($r_p<50$ nm), this stress is not realized, because the crystal does not fill the void. Instead, the curved crystal/
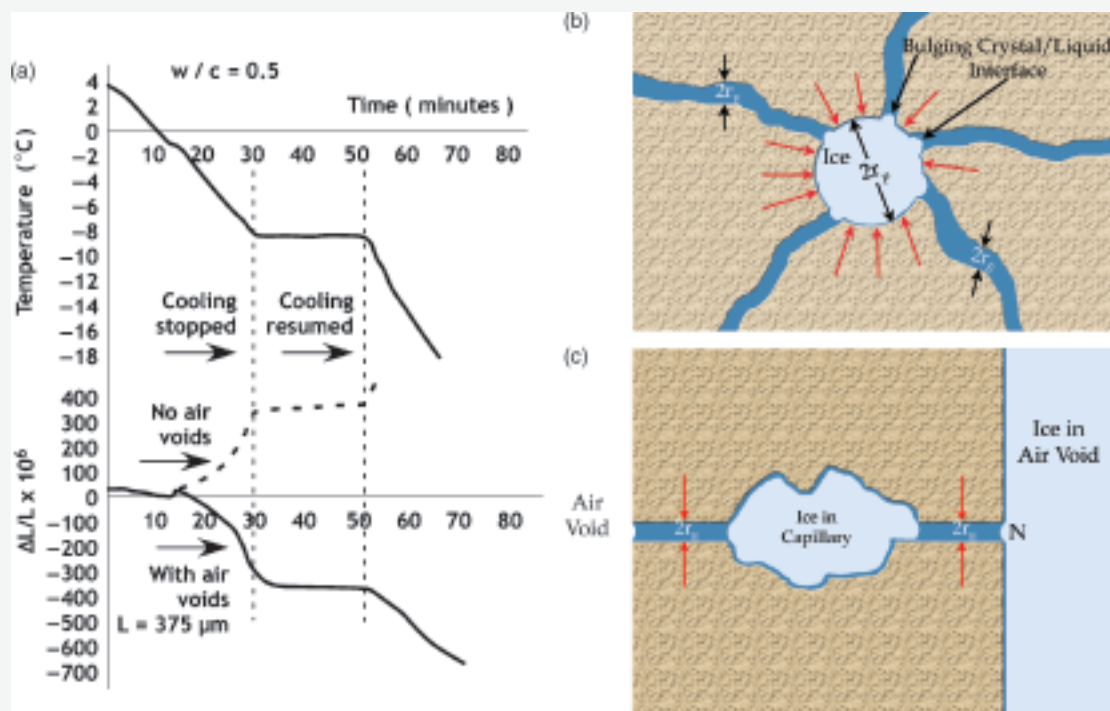

Fig. 3.   (a) Results from Powers and Helmuth[39] (Figure 2, p. 286) that indicate air voids (average spacing, $L=375$ μm) reverse the volume change realized upon freezing a cement prism. (b) Schematic of ice confined in a capillary pore ($r_p<50$ nm), but unable to penetrate the intersecting pores. The red arrows indicate the confining pressure necessary to prevent growth in the direction of the pore wall. This pressure results in a tensile hoop stress in the pore wall. (c) Schematic of ice in an air void and in a capillary pore. The negative pressure in the pore fluid next to the nose (N) pulls the solid matrix into compression, nullifying the hoop stress in the pore wall because of the crystal in the capillary pore.

Sidebar 3.   Continued

liquid interface that bulges into intersecting pores (Fig. 3(c)—N) will impose suction in the pore liquid surrounding the void, compressing the porous skeleton.[10,16,34] When the voids are intentionally entrained at a small average spacing, this suction pulls the entire solid matrix into compression, overriding the crystallization pressure in the porosity. This explains the means by which air entrainment reverses the volume change observed when a saturated concrete body is frozen (Fig. 3(a)): ordinary concrete expands, owing to crystallization pressure in the pores of the cement paste, but air-entrained concrete contracts, owing to the suction created in the pore liquid by crystals in the voids. The beneficial effect of air entrainment on both internal frost action and salt scaling has led many researchers to conclude that the same mechanisms are responsible for both types of damage. However, susceptibility to these damage mechanisms is often uncorrelated.[24,29–31,40–44] Moreover, crystallization pressure does not account for all the characteristics of salt scaling (Section *II*), most notably the pessimum concentration. When a salt solution is confined to the surface of a concrete slab, the concentration of salt in pores near the surface increases, and eventually (within days) equilibrates with the external solution. The presence of salt reduces the amount of ice formed,[12,15,45] and thus the overall volume exposed to crystallization pressure. Therefore, if crystallization pressure were important, the most damaging solution would be pure water.

expansion mismatch, ΔT is the temperature change, and throughout this section the subscripts g and e indicate quantities that correspond to the glass and epoxy, respectively. The stresses in the epoxy, σ_e, and the glass, σ_g, are

$$\sigma_e = \frac{0.5 t_g \left[E_g/(1-\nu_g) \right] \Delta\alpha\Delta T}{0.5 t_g \left(E_g/E_e \right)\left[(1-\nu_e)/(1-\nu_g) \right] + t_e} \quad (4)$$

$$\sigma_g = -2\sigma_e \left(\frac{t_e}{t_g} \right) \quad (5)$$

where t is the thickness of the constituents. Equations (3)–(5) indicate that $\sigma_{gs} = -\sigma_g$.

The same analysis can be applied to a composite of ice on the surface of a cementitious material (CM = cement paste, mortar, or concrete), where ice plays the role of the epoxy. From the dimensions normally used in a scaling experiment and the properties of ice[48,49] and cement paste[37,50] (Table I), the glue-spall stress is $\sigma_{gs} \approx 2.6$ MPa for a uniform temperature change of $\Delta T = 20°C$. This stress is capable of damaging a CM surface, especially if the surface is weakened by exposure, or if the aggregate is visible, because the interfacial transition zone (ITZ) between the aggregate and cement paste is the weakest portion of the body.[52–55]

IV. Properties of Brine Ice

The liquidus of an NaCl–H_2O solution is shown in Fig. 5. When ice forms from a saline solution, none of the solute enters the crystal lattice, so ions originally in solution are expelled into the remaining brine. Using the liquidus concentration, W_L, and the original solution concentration, W_0, the volume fraction of ice, ϕ, at a given undercooling, ΔT, can be calculated using the lever rule (Fig. 5)[56]

$$\phi = 1 - \frac{W_0}{W_L} \quad (6)$$

Any two-phase mixture of NaCl and H_2O, at a temperature below the melting point, will contain brine above the eutectic temperature, $T \approx -21°C$. Figure 5 indicates that this brine is contained in pockets encompassed by ice.[48,57,58] The same behavior is expected for the other solutes investigated in the classic scaling studies (Fig. 2),[3] because they exhibit similar melting point depressions as a function of concentration.

The pessimum concentration is explained through consideration of the effect of the brine pockets on the mechanical properties of brine ice. Freezing a moderately concentrated solution produces brine pockets that constitute flaws, which weaken the ice, rendering the ice layer prone to cracking. Cracks propagate into the surface and cause scaling. Freezing
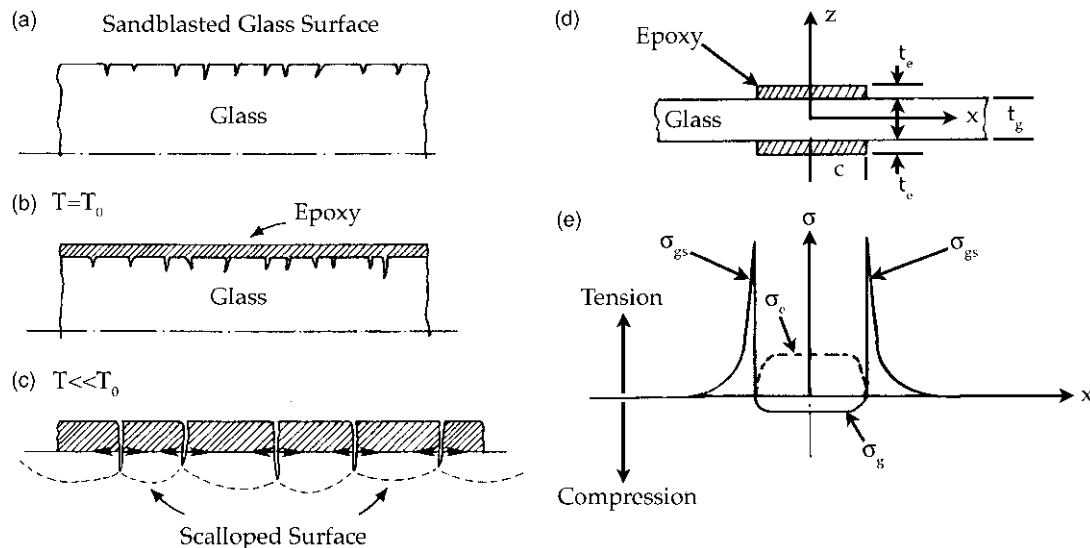

Fig. 4. (a–c) Schematic representation of the glue-spall mechanism: (a) sandblasted glass surface, (b) epoxy/glass composite at initial temperature, T_0, and (c) interface of composite, illustrating the islands of epoxy and the thin scallops of glass removed when $T \ll T_0$. (d,e) Schematic representation of an epoxy/glass/epoxy sandwich seal and the stress that arises in the composite. (d) Sandwich seal, dimensions and orientation. (e) Schematic of stress that arises in the glass surface under the epoxy, σ_g, in the epoxy, σ_e, and the glue-spall stress around the boundary of the epoxy, σ_{gs}. Figure reprinted from Gulati *et al.*[46]

Table I. Typical Values for Cement Paste,[36,37,50] Ice,[48,49] and Glass [51] Used in Warping Experiments and Salt Scaling Experiments like ASTM C672

Material	E (GPa)	v	$\alpha \times 10^5$ (°C^{-1})	t (mm)	w (mm)
Ice (f)	10	0.33	5.1	3–6	17.4
CM (c)	16.2	0.2	1	3–75	21.4
Glass (g)	57.1		0.275	3.2	25

In the text these parameters utilize subscripts. The subscripts corresponding to each material are indicated in parentheses following the material name.

more highly concentrated solutions produces ice with such high volumes of brine that the ice has no strength, so it cannot generate enough stress to cause damage to the CM.

Weeks[59] froze NaCl solutions of various concentrations and measured the tensile strength, σ_T. He found the following empirical dependence on the volume fraction of ice, ϕ:[59]

$$\sigma_T(\text{MPa}) = 2.47 - 5.15\sqrt{1 - \phi} \qquad (7)$$

Equation (7) indicates that brine ice has no strength below a volume fraction of $\phi \approx 77\%$. At the lowest temperature in a salt scaling experiment ($T \approx -20°C$), ice is in contact with brine at $W_L \approx 22\%$ (Fig. 5). Using this value in Eq. (6), setting $\phi = 77\%$, and solving for W_0, indicates that a solution with $W_0 \geq 6\%$ has no strength in the temperature range of a salt scaling experiment. Given $W_L(-10°C) = 14\%$, the same calculation indicates that a salt solution with $W_0 = 3\%$ has no strength above $T = -10°C$. Therefore, the inability of highly concentrated solutions ($W_0 \geq 6\%$) to cause scaling and the absence of damage above $T = -10°C$ are explained by consideration of how brine pockets affect the strength of brine ice.

To estimate the mismatch stress in the ice layer and predict the likelihood of cracking when $W_0 < 6\%$, it is necessary to know the elastic modulus of the frozen layer, E_f. Brine ice is a heterogeneous material with two phases, ice and porosity (pockets) filled with salt solution. Bounds on the modulus can be estimated using the composite theory of Hashin and Shtrikman,[60] which provides the best possible bounds given only the volume fractions and mechanical properties of the constituent materi-

als.[61] The 3-d solution represents a body containing a random distribution of irregularly shaped inclusions. It is applicable when ice crystals spread throughout the brine forming a porous network saturated with the remaining brine. The 2-d solution is exact for disks in a plane (aligned cylinders in 3-d), and would be most accurate for brine ice formed by unidirectional freezing, which results in parallel channels of brine. It was previously shown[62] that either bound (2- or 3-d) represents a good approximation to data for the elastic modulus of brine ice.[49,63]

Ice exhibits rapid creep, so the stress in the frozen layer depends strongly on the viscoelastic parameters for ice. The creep strain rate, $\dot{\varepsilon}_x$, is proportional to the cube of the stress, σ_x:[64]

$$\dot{\varepsilon}_x = J_{\text{Cr}}\sigma_x^3 \qquad (8)$$

The temperature dependence of creep was originally described by a series of Arrhenius fits over small ranges of temperature,[64] but we find that the Vogel–Fulcher–Tammann equation[65] provides an excellent fit over the whole temperature range of interest:

$$J_{\text{Cr}} = \exp\left(-21.183 - \frac{211.71}{T - 28.338}\right) \qquad (9)$$

V. Stress in the Ice Layer

When ice forms on a sidewalk, the stress in the ice layer is biaxial and that in the concrete is negligible, because the thickness of the ice layer is small compared with that of the concrete slab, $t_f \ll t_c$. In this situation, the elastic stress in the ice layer is given by:

$$\sigma_x = \frac{E_f}{1 - v_f}\Delta\alpha\Delta T = B_f\varepsilon_f \qquad (10)$$

where $\Delta\alpha = \alpha_f - \alpha_c$ is the thermal expansion mismatch, $\varepsilon_f = \Delta\alpha\Delta T$ is the thermal mismatch strain, $B_f = E_f/(1-v_f)$ is the biaxial modulus, and the subscripts f and c stand for the frozen ice layer and the CM, respectively. Using the properties of ice and cement shown in Table I, and setting σ_x equal to the tensile
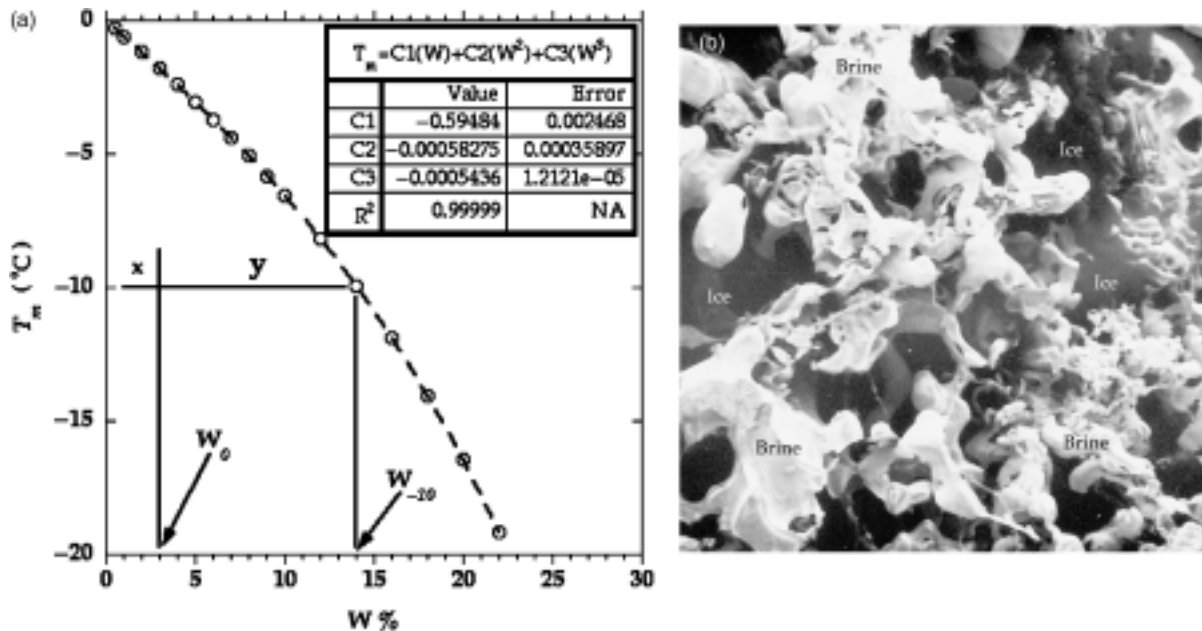

Fig. 5. (a) NaCl–H$_2$O liquidus; illustrating the lever rule (i.e., at −10°C the volume fraction of ice is determined by, $\phi = 1 - x/y = 1 - W_0/W_{-10}$). (b) Picture of epoxy impregnated brine ice, where the epoxy fills the brine pockets. Picture taken from Weissenberger *et al.*[57]

strength of ice (2.5 MPa),[59] Eq. (10) suggests that pure ice will crack at $\Delta T \approx 4^\circ C$. If this were the case, we would expect pure ice to cause scaling damage, which is not consistent with the empirical observations (Fig. 2).

This apparent discrepancy results from our neglect of creep when calculating the stress. Allowing for creep, the stress is represented by[62]

$$\sigma_x = \int_T^{T_m} B_f\left(\Delta\alpha - \frac{J_{Cr}\sigma_x^3}{\dot{T}}\right)dT \quad (11)$$

As the creep strain depends on the cube of the stress, an analytical solution for stress is not possible, so the stress must be computed iteratively. For salt solutions, this calculation is complicated by the fact that the volume fraction of ice increases as the temperature is lowered (Fig. 5). After each temperature step, the newly formed ice is stress free, and the stress in the existing ice varies based on when it was formed. The corresponding stress in the ice layer is calculated as the volume-weighted average stress[62]

$$\sigma_x^{(n)} = \frac{\phi^{(n-1)}\sigma_x^{(n-1)}}{\phi^{(n)}} + B_f^{(n)}\,dT\left[\Delta\alpha - \frac{J_{Cr}\left(\sigma_x^{(n-1)}\right)^3}{\dot{T}}\right] \quad (12)$$

where the superscript in parentheses indicates the number of the temperature steps of magnitude dT. The calculations presented here represent an improvement over the calculations in Valenza and Scherer,[62] because the stress is not permitted to arise until the volume fraction of ice is high enough to permit nonzero strength, according to Eq. (7).

The stress was calculated using Eqs. (9) and (12) for NaCl solutions of various concentrations exposed to a uniform linear temperature change between $T = 0^\circ$ and $-20^\circ C$ over 3 h. The biaxial modulus of the ice layer is calculated from the Hashin–Shtrikman bounds using the properties of ice shown in Table I, and the following properties of brine: $G_1 = 0$ and $K_1 = 2.18$ GPa.[66] The volume fraction of ice is determined by the lever rule, Eq. (6), where the initial solution concentration, W_0, is specified and the concentration of the solution in equilibrium with ice, W_L, is incrementally increased until the eutectic concentration is reached. The corresponding temperature is calculated from the fit of a third-order polynomial to data for the melting point depression of NaCl–H$_2$O solutions from Weast and Astle[66] (Fig. 5). For comparison, the elastic stress is also calculated using Eq. (10).

Results from the simulations for solutions with NaCl concentrations between 0% and 3% are shown in Figs. 6–9. The results show that creep limits the stress in the ice layer to a value below the strength, when pure water or a 1% NaCl solution is frozen on a sidewalk. In contrast, when a 2%–3% NaCl solution is frozen, the mismatch stress is greater than the strength of the brine ice, so the ice layer is expected to crack. Results for a 4% NaCl solution were similar to those for a 3% solution, with the exception that the ice layer does not gain strength until the temperature is reduced to $-14^\circ C$. The stress in a pure ice layer was calculated for three freezing rates, assuming that the temperature was reduced from 0° to $-20^\circ C$ in 1, 3, or 5 h. The calculated stress increases as the freezing rate increases, but remains below the strength (2.5 MPa) even for rapid freezing rates (1 h) that are uncharacteristic of scaling tests or natural cooling.

Over the range of concentration where brine ice is expected to crack, increasing the salt content from 2% to 4% reduces the temperature at which the brine ice gains strength, as well as the volume fraction of ice at $T = -20^\circ C$. Reducing the temperature at which the ice gains strength limits the stress that the fractured ice layer can impose during a scaling experiment, and a lower volume fraction of ice reduces the contact area between the ice and the surface. Both of these effects will result

in less scaling damage.[67] The stress that arises when the composite is formed from a 2% salt solution is marginally greater than the corresponding strength. As a result, there may be less cracking in the ice layer when a 2% solution is frozen, than when a 3% or 4% solution is frozen. Fewer cracks will also result in less scaling damage. Considering these three effects, it seems that a 3% salt solution presents the optimal situation for causing salt scaling. The 3% solution gains strength at a higher temperature and forms a greater volume fraction of ice than a 4% solution, and the stress in the ice layer is expected to be roughly twice the strength, a much greater difference than that realized with a 2% solution. The difference between the stress and the strength is relevant because strength is dictated by larger flaws; when the stress rises significantly above the strength, the propensity for propagating smaller flaws will result in more cracking.

The results from the simulation indicate that when frozen on the surface of a CM: (a) salt solutions with concentrations less than 1% are not expected to crack, (b) moderately concentrated solutions (2%–4%) are expected to crack and cause scaling, and (c) solutions of higher concentration are not expected to impose stress on the surface. This conclusion is illustrated in Fig. 10, which shows how the mechanical properties of ice account for the pessimum concentration.

VI. Fracture Mechanics

Cracking of a brittle layer on a substrate has been extensively studied using the theory of linear elastic fracture mechanics (LEFM), which requires that the fracture process zone at the crack tip is very small compared with the dimensions of the material. Concrete is quasi-brittle,[68] so the size of the fracture process zone is not negligible. However, qualitatively the conclusions drawn from the LEFM analyses are applicable, and account for both the occurrence and morphology of scaling when the ice layer is expected to crack.

(1) Crack Penetration

When the ice layer cracks, scaling can occur by two processes: (1) propagation of pre-existing surface flaws or (2) penetration of the crack from the ice layer into the surface. The former process occurs in the glue-spall technique, where flaws are introduced into glass by sandblasting. It is likely that a CM surface has pre-existing flaws from exposure and traffic, so propagation of these flaws is expected. To investigate the latter possibility, we utilize a fracture mechanics analysis of channel cracking in a film on a substrate.[69]

There are three situations that can occur when a film cracks on a substrate (Fig. 11): the crack can arrest at the interface, it can bifurcate along the interface, or it can penetrate the substrate. A crack will bifurcate along the interface only if the bond between the film and the substrate is weak. Experimental evidence indicates that the bond between ice and hydrophilic surfaces is greater than the strength of ice itself, owing to the mechanical interlocking between the two materials.[67] This is especially likely for a cementitious surface, which offers greater roughness than the metal surfaces on which this trend was demonstrated.

To predict whether a crack in the ice layer will penetrate the substrate, one only needs to know the elastic properties and fracture toughness of the constituent materials. The elastic mismatch in a system consisting of a film on a substrate is characterized by the Dunder's parameter, β_D:[69]

$$\beta_D = \frac{(1-\nu_c)/G_c - (1-\nu_f)/G_f}{(1-\nu_c)/G_c + (1-\nu_f)/G_f} \quad (13)$$

where the subscripts c and f, stand for cementitious (CM substrate) and film (ice layer), respectively. Using the parameters for hardened cement paste and ice shown in Table I, and $G = E/$
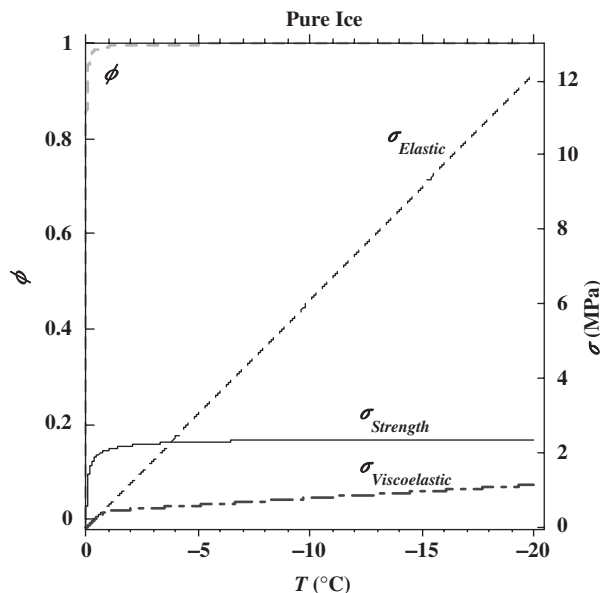
Pure Ice

Fig. 6. Calculated stress ($\sigma_{Viscoelastic}$) in a pure ice layer on a sidewalk. Creep prevents the stress from rising above the strength, whereas the elastic stress rises above the strength at an undercooling of $\Delta T \approx 4°C$.
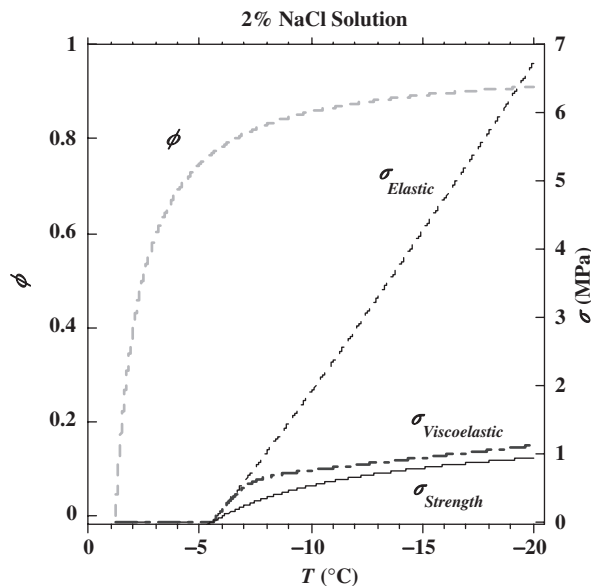
2% NaCl Solution

Fig. 8. Calculated stress ($\sigma_{Viscoelastic}$) in the ice layer when a 2% NaCl solution is frozen on a sidewalk. Creep reduces the stress well below the elastic stress, but does not prevent the stress from rising above the strength.

$2(1+\nu)$, the Dunder's parameter for an ice/cement paste composite is $\beta_D \approx -0.2$.

The fracture toughness, K_{Ic}, of the constituent materials is shown in Fig. 12, and the fracture energy, Γ, is related to the fracture toughness by $\Gamma = K_{Ic}^2/E$. The gray bar along the abscissa represents the ratio of fracture energies that correspond to the low end of the reported range of fracture toughness for cement paste ($K_{Ic} \sim 0.1$–0.5 MPa $\cdot$ m$^{0.5}$).[55,70] Considering only the lower portion of this range is not overly pessimistic, because the surface is the weakest part of the CM, because of bleeding, finishing, and drying.[71–74] The effect of drying is pertinent, because most scaling experiments recommend a period of drying in laboratory air before testing, and drying causes microcracks. Moreover, once a crack penetrates the surface of concrete, the ITZ between the aggregate and the paste will govern the fracture process, because the ITZ has a toughness on the order of 0.1 MPa $\cdot$ m$^{0.5}$.[55] For this range of toughness, Fig. 12 indicates that the crack will penetrate the cement paste up to a depth of 0.75 times the thickness of the ice layer.

(2) Crack Trajectory

The mechanics of film spalling have been investigated thoroughly.[75–77] With respect to salt scaling, these analyses are of interest, because they account for the damage morphology. Consider the situation illustrated in Fig. 11(c), where the split in the film penetrates the underlying substrate. After the crack reaches a critical depth, it deflects into a trajectory parallel to the interface. The mechanics of the fracture process account for this trajecto-
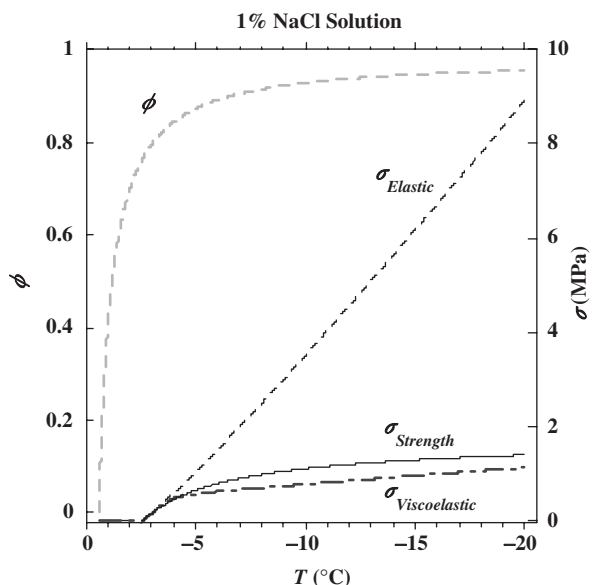
1% NaCl Solution

Fig. 7. Calculated stress ($\sigma_{Viscoelastic}$) in the ice layer when a 1% NaCl solution is frozen on a sidewalk. Creep prevents the stress from rising above the strength.
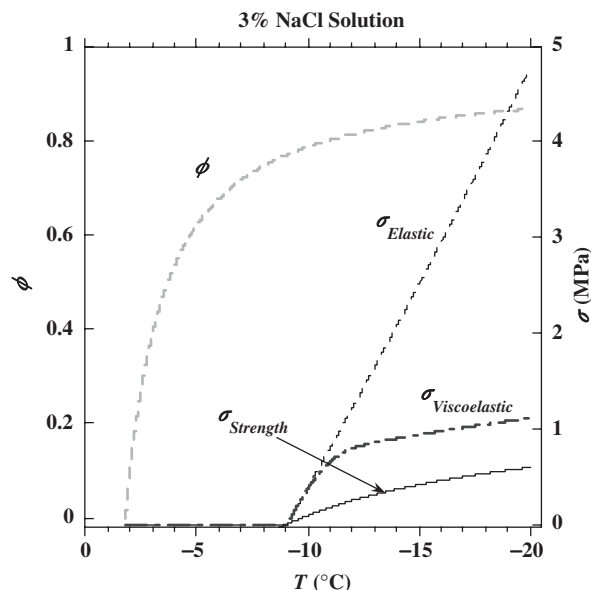
3% NaCl Solution

Fig. 9. Calculated stress ($\sigma_{Viscoelastic}$) in the ice layer when a 3% NaCl solution is frozen on a sidewalk. Creep reduces the stress below the elastic stress; however, the stress is still well above the tensile strength.
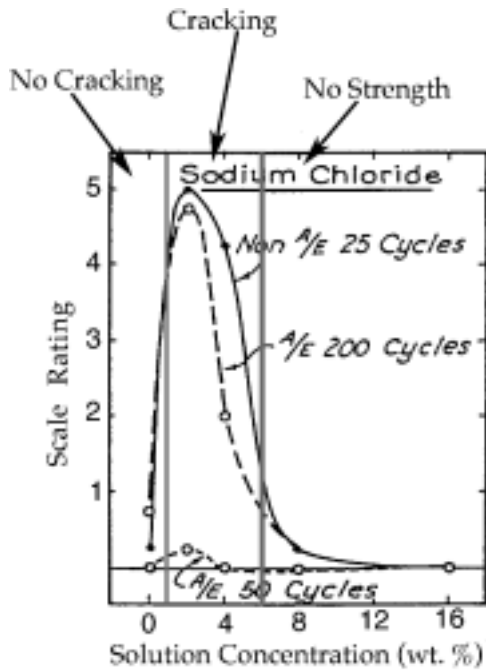
Fig. 10. Results from the classic scaling study reported in Verbeck and Klieger[3] (Figure 2, p. 3), illustrating the pessimum concentration. The schematic illustrates how the mechanical and viscoelastic properties of the ice layer account for the pessimum concentration.

Fig. 12. Plot of the depth of crack penetration for several values of the Dunder's parameter, β_D. The gray bar along the abscissa represents the lower 25% of the range of fracture toughness reported for cement paste in Mindess and Young.[55] The corresponding gray bar on the ordinate indicates the expected depth of crack penetration for the range of cement paste K_{Ic} indicated. Figure from Ye et al.,[69] reprinted with permission from Elsevier.

ry, and provide a means for predicting the likelihood of crack propagation parallel to the interface.

When the substrate is much thicker than the film, the mode I stress intensity, K_I, for a line force on a crack surface is[75]

$$\frac{K_I}{\sigma_0 \sqrt{t_f}} = \frac{2.6}{\sqrt{\pi \omega}} \tag{14}$$

where $\omega = t_f(d - t_f)$. Equation (14) indicates that the stress intensity for crack penetration decreases as the crack depth (d) increases, because the driving force for crack penetration is the mismatch stress at the interface.[69,76] The mode I stress intensity for a crack parallel to the interface is[75]

$$\frac{K_I}{\sigma_0 \sqrt{t_f}} = \frac{0.434}{\sqrt{\Sigma + \omega}}$$
$$+ \frac{0.966\omega(1 + \omega)}{\sqrt{(\Sigma + \omega)\left[\Sigma^2 + \omega^4 + 2\Sigma\omega(2 + 3\omega + 2\omega^2)\right]}} \tag{15}$$

where $\Sigma = E_f/E_c$. Equations (14) and (15) are plotted in Fig. 13 for the ice/cement paste system, which illustrates that the

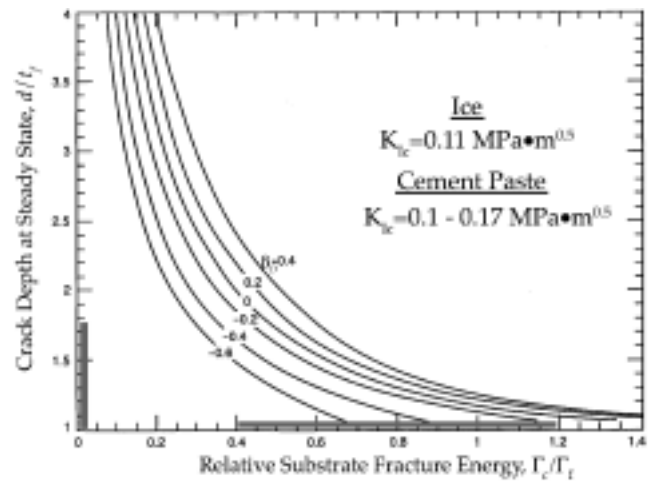propensity for crack propagation parallel to the interface is greater than that for penetration once the crack reaches a critical depth.

The crack becomes parallel to the interface at a depth where the mode II stress intensity is zero, $K_{II} = 0$[75–77]:

$$\frac{K_{II}}{\sigma_0 \sqrt{t_f}} = \frac{0.558}{\sqrt{\Sigma + \omega}}$$
$$- \frac{0.752\omega(1 + \omega)}{\sqrt{(\Sigma + \omega)\left[\Sigma^2 + \omega^4 + 2\Sigma\omega(2 + 3\omega + 2\omega^2)\right]}} \tag{16}$$

For an ice/concrete composite with $t_f \approx 6.5$ mm and $\Sigma \approx 8/25$, the mode II stress intensity goes to zero when $\omega \approx 0.7$, which corresponds to a depth of approximately 4.2 mm. The mode I stress intensity for a crack parallel to the interface at this depth, according to Eq. (15), is $K_{Ic} \approx 0.1$ MPa·m$^{0.5}$. This value is on the low end of the range of fracture toughness of CM (Fig. 12), but it is representative of the ITZ.[55] It is known that cracks in CM propagate preferentially through the ITZ,[54,55] and it was recently reported that scaling cracks circumscribe the aggregate particles.[4] A finite element simulation of ice cracking on concrete also indicates that the cracks pass through the ITZ.[34] Thus, the occurrence and morphology of scaling damage are consistent with the LEFM analysis.
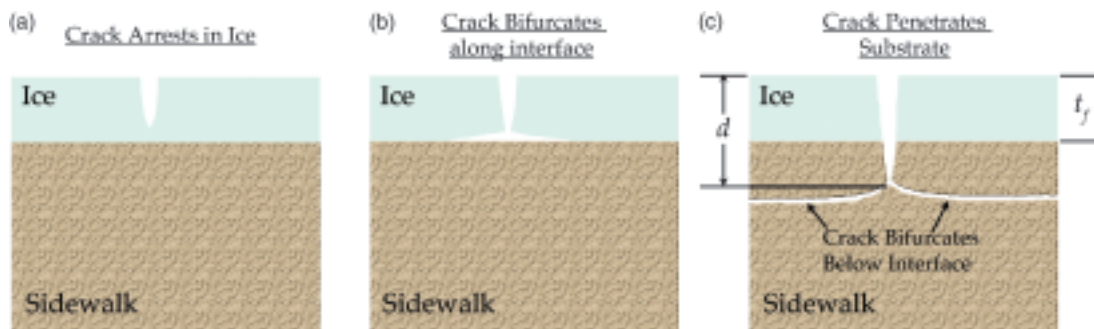

Fig. 11. Illustration of the three situations that may occur when the ice layer cracks from the mismatch stress. The crack may (a) arrest in the ice, (b) bifurcate along the ice/cement interface, or (c) penetrate the cement surface.
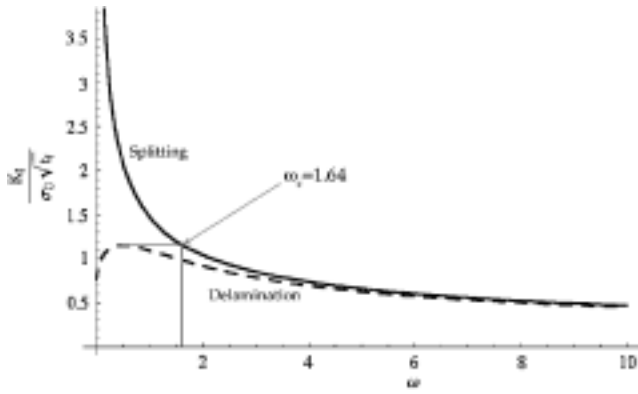
Fig. 13. Plot of Eqs. (12) and (13), with $\Sigma = 8/25$ showing the stress intensity factor for crack penetration (splitting) and crack growth parallel to the interface (delaminate). The plot shows that when the surface crack reaches a critical depth, the stress intensity for delamination is greater than that for splitting.

VII. Experimental Procedure

In this section, we describe a series of experiments that prove the importance of thermal expansion mismatch stress between ice and CM. The frozen layer is shown to crack only when a small amount of solute is present, and cracking of the ice leads to damage in the surface of the CM. The experimental method is to freeze a layer of brine on a thin plate of cement paste, and to determine the resulting stress from the bending of the ice/CM composite. Details of the procedure are reported elsewhere.[10,51]

(1) Bi-Material Effect

Timoshenko derived an expression for the radius of curvature, ρ, of a bi-material composite exposed to a uniform temperature change, ΔT[79,80] (in the present case, T is the undercooling below the liquidus temperature, T_L):

$$\frac{1}{\rho} = \frac{\Delta \varepsilon_f K_R}{h} \tag{17}$$

$$\Delta \varepsilon_f = \int_{T_L}^{T} (\alpha_1 - \alpha_2)\, dT = \Delta \alpha \Delta T \tag{18}$$

$$K_R = \frac{6(1 + m^2)mnl}{1 + 4mnl + l^2 m^4 n^2 + 6m^2 nl + 4m^3 nl} \tag{19}$$

where t is the layer thickness, E is the elastic modulus, w is the width, and the subscripts 1 and 2 indicate quantities that correspond to the top and bottom layers, respectively; $h = t_1 + t_2$ is the thickness of the composite, $m = t_1/t_2$, $n = E_1/E_2$, $l = w_1/w_2$. Equations (17)–(19) are derived following the method of Timoshenko, but allowing for different layer widths.

If the bi-material strip is simply supported (Fig. 14), the deflection due to a uniform temperature change, ΔT, is determined by approximating the curved composite as a portion of the circumference of a circle with radius, ρ. This geometrical representation is illustrated in Fig. 14(b), which indicates that $b = \rho - \delta$. The Pythagorean theorem yields $\delta(2\rho - \delta) = (W_B/2)^2$; therefore, when $\delta < < \rho$, the deflection is related to the curvature by

$$\delta = \frac{W_B^2}{8\rho} = \frac{W_B^2}{8} \frac{\Delta \varepsilon_f K_R}{h} \tag{20}$$

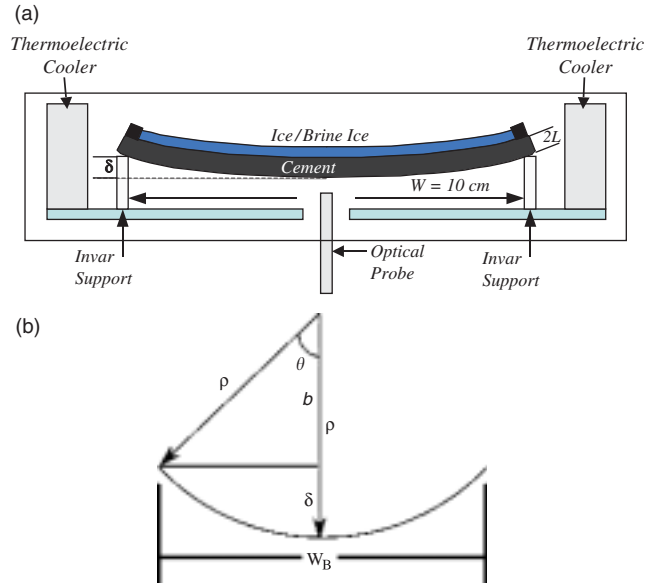where the second equality follows from Eq. (17).

(a)

(b)

Fig. 14. (a) Schematic of the warping experiment. The experiment consists of simply supporting a thin plate of cement paste, confining a pool of fluid to the surface of the plate, and exposing the system to a temperature cycle. (b) Geometrical representation of bi-material bending.

(2) Warping Experiment

Figure 14 shows a schematic of the apparatus used to detect the deflection caused by freezing a pool of solution on a thin CM plate. The sample sits above an optical probe that measures the movement of the bottom of the CM with a sensitivity of $\sim 1\ \mu m$. Two thermoelectric coolers are used to control the temperature. Inside the apparatus, the sample is simply supported by two invar T-supports that are anchored to an invar plate. The temperatures inside the box, in the solution on the sample surface, and that of the optical probe are monitored by thermocouples.

(3) Freezing Saline Solutions

Owing to the effect of brine pockets on the mechanical properties of ice, the propensity for ice to crack varies with the initial solution concentration. Empirical evidence of this effect was obtained by freezing solutions held in a glass cup with a cold stage. The bottom of the cup was sandblasted to promote adhesion between the ice and the glass. A video of the experiments was recorded through an optical microscope.

VIII. Experimental Results

(1) Warping Experiment

(A) Pure Water: Results from a warping experiment with a cement paste plate ($t_c = 2.7$ mm), and pure water are shown in Fig. 15. After solidification of the pool, a cement paste/ice bi-material composite is formed. The thermal expansion coefficient of the ice layer is five times that of the cement paste (Table I). Figure 15 illustrates that as the temperature is reduced below the melting point ($T_m = 0°C$), the composite exhibits a concave upward deflection. The deflection expected from a uniform temperature change is determined from the radius of curvature using Eqs. (17)–(20). With the values in Table I, the expected deflection is $\sim 12\ \mu m/°C$. The observed deflection (Fig. 15—indicated by arrows) is 8–10 $\mu m/°C$. The discrepancy between the expected deflection and that observed results from creep in the ice layer.

The ice creeps during an isotherm after a temperature change. Figure 15 shows that allowing for creep yields good agreement between the predicted and observed deflection. This is an *a priori*
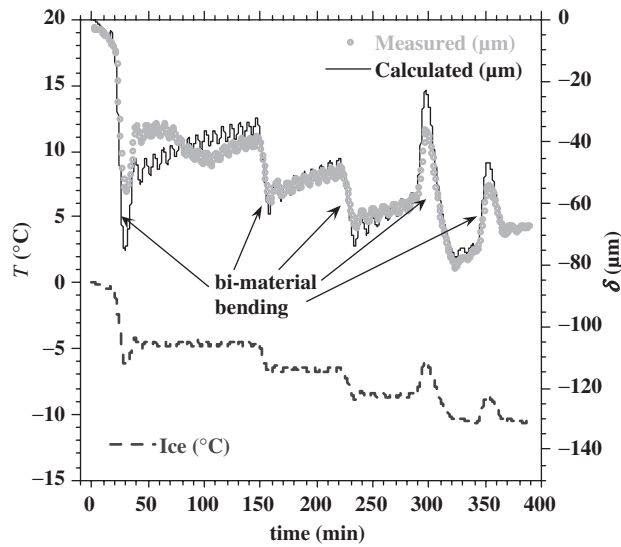
Fig. 15. Results from warping experiment with pure water after nucleation and subsequent temperature reduction. Accounting for creep in the ice layer, the calculated curve reproduces all the characteristics of the observed deflection. The discrepancy observed between the measured and calculated deflection during the first temperature step is most likely because of slippage at the interface, which would also explain the instability at $t = 70$ min.

prediction of the deflection using the material properties shown in Table I and creep data for ice from Barnes *et al.*[64] (Eq. (9)). The analysis assumes a perfect bond between the two materials. Therefore, the large discrepancy between the measured and calculated deflection corresponding to the first temperature reduction (Fig. 15) is most likely related to imperfect adhesion between the ice layer and the cement paste. The latter effect is only active at higher temperatures ($T > -5°C$),[67] and may also account for the instability in the deflection after the first temperature change.

To test our creep calculations,[64] warping experiments were performed with a borosilicate glass plate and pure water. The surface of the plate was sandblasted to promote good adhesion. The expected deflection was calculated using the properties of ice and glass shown in Table I, and creep in the ice layer was accounted for with Eqs. (8) and (9). The elastic modulus and linear thermal expansion coefficient of the glass were measured by beam bending and dilatometry, respectively.[51] Good agreement was observed[51] between the measured deflection and that predicted using the reported creep data.[64]

Attempts were made to determine the effect of salt on the creep rate. However, owing to the stiffness of the glass plate, and the effect of brine pockets on the strength of the ice layer, no deflection was detectable. When the ice layer fails, there is no observable deflection, because cracking relieves the mismatch strain that leads to bi-material bending. This effect was verified by dividing a pure ice layer into several compartments, and then monitoring the corresponding deflection during a warping experiment. As the number of islands increases (from 1 to 28), the observed deflection disappears;[51] correspondingly, as the number of cracks in a frozen brine increases, the deflection decreases.

(B) Salt Solutions

(a) One Percent NaCl Solution: The results from a warping experiment with a cement paste plate ($t_c = 2.7$ mm) and a 1% NaCl solution are shown in Fig. 16(a). The initial deflection ($\delta \approx 60$ μm) is attributed to salt swelling (see sidebar 4, Salt Swelling).

The plot illustrates the occurrence of limited bi-material bending after the temperature is reduced to $-7.5°C$. It was shown in Section *V* (Fig. 7) that the strength of the ice layer is not expected to rise significantly above the stress until $T < -6°C$. Accordingly, Fig. 16(b) shows that the bi-material effect is first observed in the form of oscillations in the deflection corresponding to oscillations in the ice temperature around $T = -7.5°C$. Subsequent temperature reductions result in additional bi-material bending.

(b) Three Percent NaCl Solution: The results from a similar experiment with a cement paste plate ($t_c = 2.86$ mm) and a 3% NaCl solution are shown in Fig. 18. Before nucleation, the baseline drifts by ~ 50 μm over a period of 210 min. This is in very good agreement with the deflection observed during the salt swelling warping experiments, shown in Fig. 17. At $t = 234$ min, ice nucleates in the pool, and the temperature rises to $-1.75°C$, which is the melting point of this solution.[91]
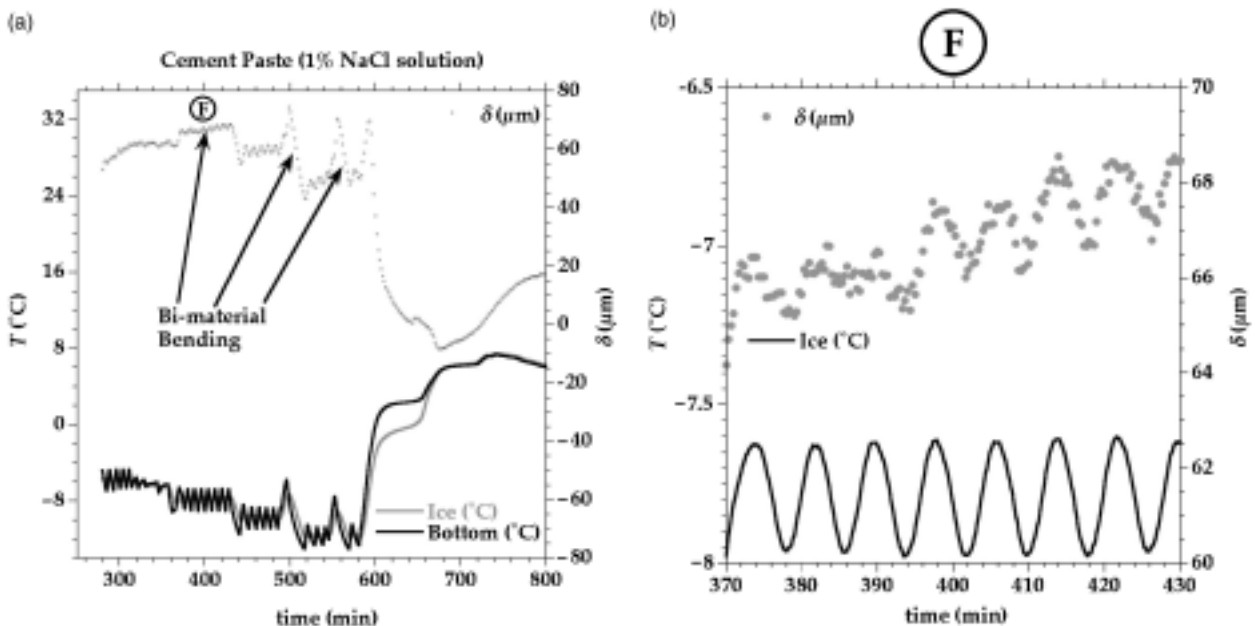

Fig. 16. (a) Warping experiment with cement paste plate ($t_c = 2.7$ mm) and 1% NaCl solution illustrates bi-material bending after the temperature is reduced to $-7.5°C$. (b) Exploded view of point (F) in (a) shows that after the temperature is reduced to $T = -7.5°C$, there are oscillations in the deflection that correspond to oscillations in the temperature. The theoretical calculation of the stress in the ice layer performed in Section *V* indicates that the strength will not rise significantly above the stress, until the temperature is reduced to $T < -6°C$, as observed.

Sidebar 4. Salt Swelling

The depth at which the salt concentration in the pore fluid will equilibrate with that in the pool on the surface is estimated from $x^2 = Dt$, where x is the equilibrated depth, D is the diffusion coefficient, and t is the time. At room temperature, the diffusion coefficient of the chloride ion in cement-based materials is known to be 10^{-11}–10^{-10} m^2/s.[81] Assuming that the diffusion coefficient of the sodium ion is similar, it is expected that the concentration of salt in the first 2–5 mm of a concrete surface will equilibrate with that of an external solution in 2–3 days. When the ions from a dissociated chloride salt enter the microstructure, cement expands.[82] The alkali ions are bound, reversibly, by deprotonated silanols[83,84] in the C–S–H gel. Chloride is irreversibly bound,[85] and several studies have shown that Cl$^-$ can exchange for OH$^-$ in aluminate phases in cement paste.[86,87] Recent XRD analysis indicates that exposure of cement paste to chloride salts results in the precipitation of Friedel's salt in any case where expansion is observed.[88,89] It has been reported that the basal spacing of the C–S–H increases upon exposure to chloride salts.[90] At present, it is still unclear whether the expansion that accompanies exposure to chloride salts is caused by swelling from ion exchange or crystallization pressure from the precipitation of Friedel's salt. When the slab of CM is thin, expansion of the surface causes the plate to warp concave down. Figure 17 demonstrates this effect and indicates that increasing the concentration of the external solution results in faster initial warping rates and a greater maximum deflection. Companion measurements indicate that upon exposure to a 21 wt% NaCl solution in water, the maximum swelling strain is $\varepsilon_{ss} \approx 5.6 \times 10^{-4}$. This strain is reached after submersion of a 3 mm cement paste plate for $t \approx 2800$ min. The maximum strain is not achieved until the entire porous network swells from exposure to the salt ions, so $D \approx L^2/t \approx 1.3 \times 10^{-11}$ m^2/s, which is within the expected range for chloride diffusion in cement paste.[81] During a scaling experiment, the CM surface is exposed to a concentration close to the eutectic ($\sim 22\%$ NaCl) at the minimum temperature ($T \approx -20°$C) for a period of 4–6 h. Over six hours, it is expected that the salt concentration in the surface will equilibrate with the external concentration to a depth of 0.5–1.5 mm. As the thickness of the surface that swells is small compared with the dimensions of the concrete sample, the swelling is totally suppressed and a biaxial compressive stress arises in the surface:

$$\sigma_x = -\frac{E}{1-\nu}\varepsilon_{ss} \qquad (21)$$

Assuming a typical value for the elastic modulus of the CM, $E = 13$–19 GPa, and the Poisson's ratio, $\nu = 0.2$, Eq. (21) indicates that the compressive stress is $\sigma_x = 9$–13 MPa. This stress is below the reported range for the compressive strength of CM, 25–45 MPa,[54] but it may weaken the surface by causing buckling over defects or aggregate, rendering it more susceptible to salt scaling. It is unlikely that salt swelling is the primary cause of scaling damage. In particular, salt swelling does not account for the pessimum concentration or the similar effect of chemically dissimilar solutes. Moreover, the formation of Friedel's salt and the related damage are not observed when cement paste is exposed to chloride solutions at low temperature ($T < 0°$C).[51] However, in practice, NaCl and CaCl$_2$ are regularly used to de-ice roadways and walkways, and the stress resulting from this exposure may render a CM surface more susceptible to salt scaling.
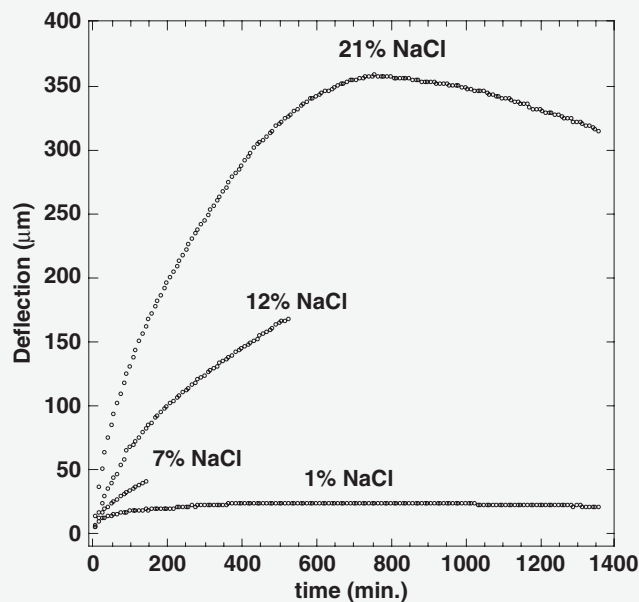

Fig. 17. Results from warping experiments, performed at room temperature, with 3 mm thick cement paste plates using NaCl solutions of varying concentrations. The results illustrate that increasing the concentration of NaCl results in higher warping rates, and greater maximum deflection.

During the remainder of the experiment, the ice layer is incapable of causing bi-material bending, because the brine ice does not gain strength until $T \approx -9°$C.[59] The same observations were made during a similar experiment with a 7% NaCl solution.

The mechanical response during a warping experiment provides insight into the mechanisms active when a pool of solution is frozen on the surface of a cementitious body, and the effect of salt on the dominant mechanism. The results obtained with pure water illustrate bi-material bending after freezing. Experiments run with salt solutions indicate the occurrence of salt swelling. The absence of bi-material bending with the 3% and 7% NaCl solutions is expected from consideration of the temperature at which these solutions gain strength: a 3% NaCl solution is not expected to gain strength until $T = -9°$C, and a 7% NaCl solution will not gain strength above $-20°$C, but in these experiments the minimum temperature was $T = -10°$C. Accordingly, none of the samples used in these experiments was damaged. Therefore, these experiments confirm the stress calculations presented in Section V, but do not demonstrate the mechanisms responsible for salt scaling. For this purpose, warping experiments were performed using a thermal cycle extending to a lower temperature ($-18°$C), as explained in the next section.

(C) Comparative Experiments (Low Temperature): The results from the experimental series on cement paste ($t_c \approx 6.5$ mm) are shown in Fig. 19. The results indicate a clear difference in the mechanical response after freezing of brines containing 0% or 3% NaCl. In the case of pure water, bi-material bending (concave up) is observed. In contrast, the composite formed by freezing the salt solution exhibits a fairly constant rate of deflection (concave down) after freezing, where a maximum deflection of 465 μm is achieved. Owing to the low temperature, it is not expected that this deflection is caused by salt swelling (see sidebar 4, Salt Swelling). The deflection is attributed to ice that wedges open and propagates cracks created by the glue-spall mechanism (see sidebar 5, Ice Wedging); the strain is enhanced by creep of the CM[37,94,95] and by loss of stiffness as damage increases. In Fig. 21, it is shown that the difference in mechanical response is accompanied by a drastic difference in damage. The sample exposed to the thermal cycle with pure water is not visibly damaged, while the 3% NaCl solution destroys the sample surface. The morphology of damage is identical to that expected from salt scaling, and the crack trajectory is exactly that predicted by the fracture mechanics analysis in Section VI.
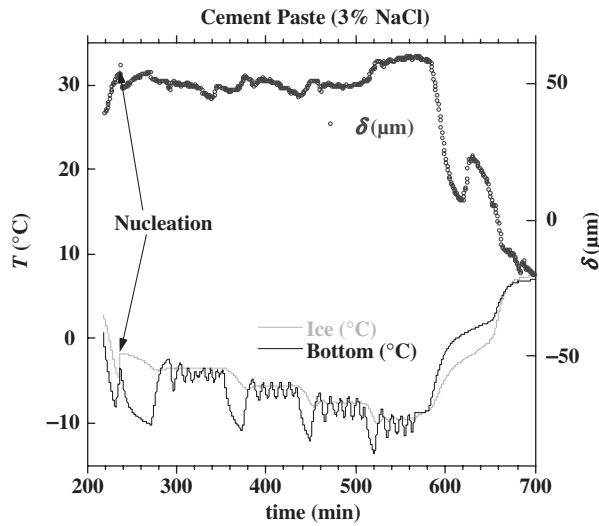
Fig. 18. Warping experiment with cement paste plate ($t_c = 2.86$ mm) and a 3% NaCl solution. Before nucleation, the baseline drifts by ~ 50 µm owing to salt swelling. After nucleation, the ice layer is incapable of causing bi-material bending.

The only noticeable difference between the experiments with cement and mortar is that the scaling damage is finer when mortar is used (Fig. 22). Cracks tend to propagate through the ITZ, because it is weaker than the remainder of the matrix,[52–54] so the damage takes the form of thin flakes of cement that may contain aggregate, or aggregate particles alone.

(2) Damage from the Glue-Spall Mechanism
The warping experiments indicate that moderately concentrated (>3% NaCl) brine or a compartmentalized ice layer is incapable of causing bi-material bending. In this section, it is verified that this similarity is related to fracture of the brine ice layer, and that the glue-spall mechanism is responsible for the corresponding damage.

(A) Microscopy, Saline Solutions: Freezing was directly observed by putting the solution of interest in a glass cup in a cold stage on an optical microscope. The bottom of the glass cup was sandblasted to promote adhesion. Figure 23 shows a still photo taken from the video of an experiment with pure water when the temperature of the water was $T \approx -18°$C. Air bubbles

and grain boundaries are clearly visible in the photo, but there is no evidence of cracking.

Figure 24 shows two still photos, taken nearly 1 s apart, from an identical experiment with a 3% NaCl solution when the temperature was $T \approx -18°$C. The ice is cracked, and comparison of the top and bottom photos illustrates crack propagation. Identical experiments were performed with more highly concentrated solutions (7%–10%), and no evidence of cracking was observed. As explained earlier, no cracking is expected in the more concentrated solutions, because the solids content is too low to allow stress build-up. An identical experimental series with ethanol solutions revealed the same trend. Cracking of the ice is not expected to cause spalling of the glass cup, according to the LEFM analysis, because the glass is too strong.

(B) Warping Experiment, Pure Water Ice in Compartments: To test the prediction that a cracked ice layer results in surface cracking from the glue-spall mechanism, we performed warping experiments with cement paste and pure water, where the water was separated into compartments (Fig. 25). The intention was to mimic failure of the ice layer, and observe the corresponding effect on the deflection as well as to investigate the occurrence of surface cracking. The results from these experiments indicate that the compartmentalized ice is initially capable of imposing bi-material bending. However, as the temperature is further reduced, the bi-material bending abruptly stops, and is followed by a rapid concave down deflection. The latter deflection is attributed to ice wedging (see sidebar 5, Ice Wedging) in surface cracks created by the glue-spall mechanism. The maximum deflection obtained was ~ 125 µm, and the peak and subsequent decrease in the deflection is related to failure of the sample (Fig. 25).

The temperature at which the bi-material effect is overcome by ice wedging is related to the thickness of the ice islands. For ice islands that were roughly 1, 2, or 3 mm thick, the bi-material response arrested at $T = -8.3°$, $-7.3°$, and $-6.3°$C, respectively. This trend is consistent with the relationship between the glue-spall stress, σ_{gs}, and the thickness of the ice islands, t_f, which corresponds to t_e in Eq. (4).[46] As the thickness of the islands decreases, the stress in the ice increases and the glue-spall stress decreases, because when the ice is very thin, it is incapable of deforming the cement paste. Using the properties for ice and cement paste shown in Table I, and the thickness of the ice islands and corresponding undercooling noted above, Eqs. (3) and (4) indicate that bi-material bending is arrested by ice wedging after surface cracks are opened by a glue-spall stress in the range 1.5–2.5 MPa. This range is in excellent agreement
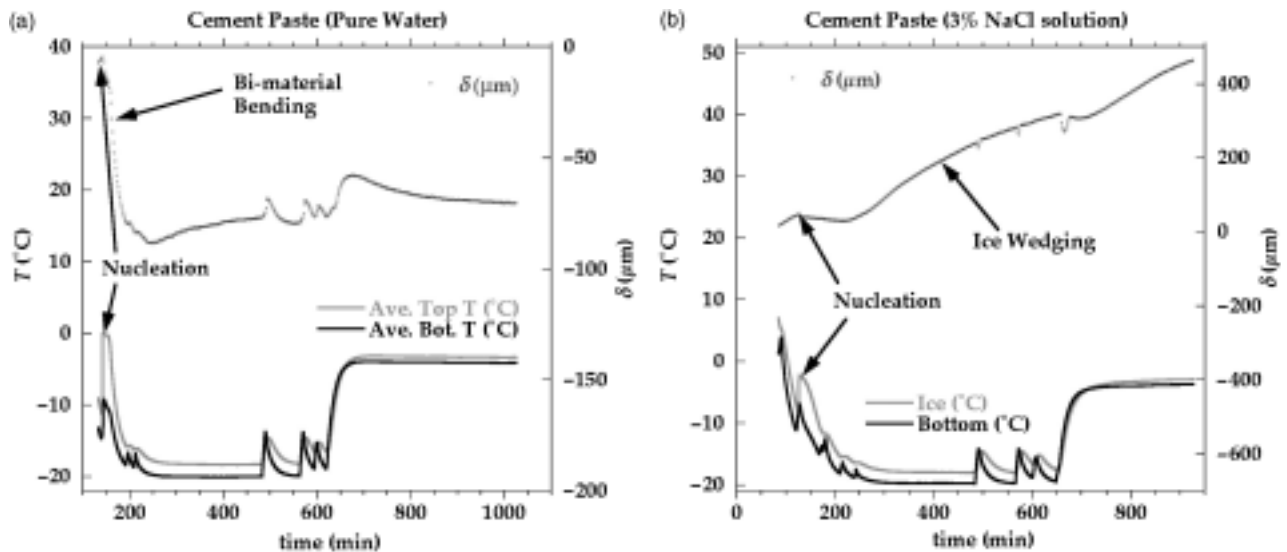

Fig. 19. Warping experiments with cement paste plates ($t_c \approx 6.5$ mm) and (a) pure water or (b) 3% NaCl solution. The pure water composite exhibits a distinct bi-material response, while the 3% NaCl composite exhibits a constant concave down deflection that is attributed to ice wedging, creep, and a reduction in the effective thickness because of scaling damage (Fig. 20).

Sidebar 5. Ice Wedging

Ice wedging occurs when ice fills a crack and pushes the faces apart (Fig. 20). When a crack forms, a film of pore solution spreads over the fracture surface; as soon as it touches the ice at the original surface, ice spreads along the fracture surface, and extracts more liquid from the pores. Owing to the small volume of the crack, it will quickly fill with ice, which will wedge the crack open. When the ice forms, it maintains a film of water between itself (see sidebar 3, Internal Frost Action) and the fracture surface. The crystal bulges into the mouths of the pores of the paste, as indicated in Fig. 20(b), until the curvature of the water/ice interface, κ_{CL}, satisfies the Gibbs–Thomson Equation (see sidebar 3, Internal Frost Action—Eq. (2)). At any point along the interface where the curvature differs from that in the pore, a pressure, P_A, must be applied on the ice by the fracture surface to suppress crystal growth[10]:

$$P_A = \gamma_{CL}\left(\kappa_{CL}^{(N)} - \kappa_{CL}^{(S)}\right) \tag{22}$$

At the shoulder and along the opposite fracture surface, where the interface is flat ($\kappa_{CL}^{(S)} = 0$), the pressure is $P_A = \gamma_{CL}\kappa_{CL}^{(N)}$. In Scherer and Valenza[10] it is shown that $\gamma_{CL}\kappa_{CL}^{(N)} = \Delta S_{fv}\Delta T$; for water, $\Delta S_{fv} = 1.3\,\text{J}\cdot\text{cm}^{-3}\cdot\text{K}^{-1}$,[92] so $P_A = \Delta S_{fv}\Delta T = 1.3\Delta T$ MPa over the area corresponding to both shoulders (S) and the opposite fracture surface. The mode I stress intensity at the crack tip for an edge crack with uniform loading (P_A) on the fracture surface is[93]

$$\frac{K_I}{\sqrt{a_c}} = 1.98\,P_A = 2.6\Delta T\,\text{MPa}\cdot\text{m}^{0.5} \tag{23}$$

where a_c is the crack length. The fracture toughness of cement paste is 0.1–0.5 MPa$\cdot$m$^{0.5}$,[56,70] so Eq. (23) indicates that ice wedging will result in crack propagation at a very small undercooling. Equation (23) assumes that the material in question is brittle, whereas cement paste is quasi-brittle,[68] so Eq. (23) is only semi-quantitative. However, it is safe to assume that crack propagation will occur from ice wedging at a small undercooling. In the presence of brine ice, the cracks from the glue-spall stress will fill with brine from the pockets breached by fracture in the ice layer. The corresponding brine ice is unable to impose a significant stress on the fracture surface because the driving force for ice growth is suppressed by the presence of the solute. However, over time this ice will extract liquid from the surrounding microstructure diluting the saline solution surrounding the ice. As the salt concentration decreases, the driving force for ice growth, and thus the stress imposed on the fracture surface increases. The longer the ice sucks moisture from the surrounding microstructure, the greater the stress and thus the propensity for crack propagation. This interpretation is supported by a limited amount of experimental evidence that suggests that prolonging the freezing period results in more salt scaling.
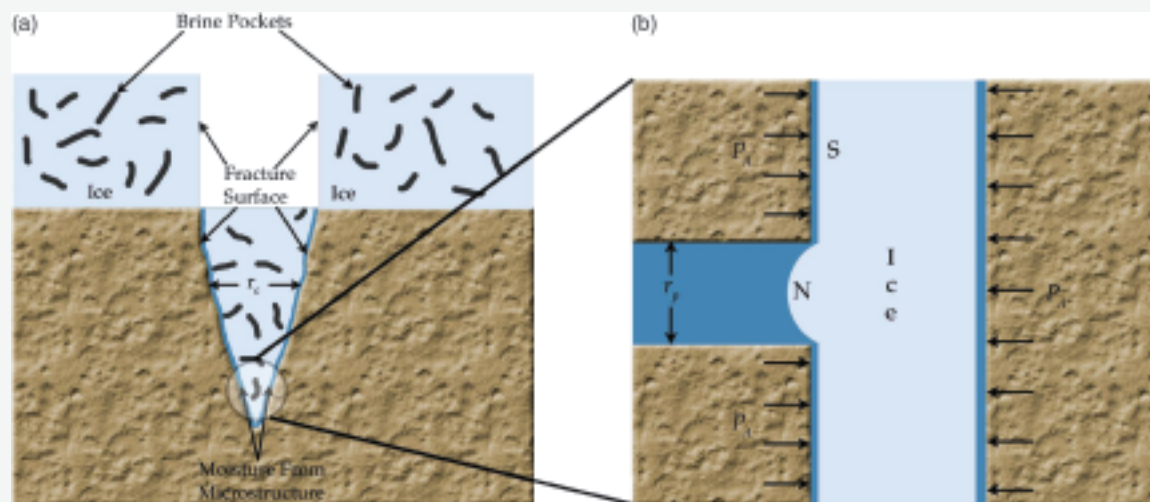

Fig. 20.   (a) Schematic of ice that forms in a crack. (b) Ice crystal bulges into a pore intersected by the crack at N. The interfacial curvature at N is determined by the undercooling, ΔT. The difference in curvature exhibited between N and S necessitates a pressure of P_A (MPa) = 1.3ΔT to suppress crystal growth at S.

with that expected to result in microcracking of cement paste, which has a tensile strength of ~3 MPa. Moreover, as discussed previously, the sample surface is expected to be the weakest zone of the body, so a stress of this magnitude is likely to cause damage.

The glue-spall stress imposed on the surface around the perimeter of the ice islands should lead to edge cracking that circumscribes the island. To investigate the occurrence of surface cracking from this mechanism, the area under the vacuum grease partitions (Fig. 25) was analyzed with an optical microscope immediately after completion of the warping experiment. Figure 26 shows the perimeter of an ice island, which corresponds to the area stained by vacuum grease. The top of the

picture corresponds to the vacuum grease line bisecting the sample along its length (Fig. 25). The picture clearly illustrates the occurrence of surface cracking that circumscribes the ice island. In addition, some of the surface laitance is removed by the shear stress at the interface. Cracking was also observed under the vacuum grease dam along the entire perimeter of the sample surface (Fig. 25). Figure 26 shows an edge view of a crack that intersects the sample edge; as expected from the fracture mechanics analysis (Section VI), the crack bifurcates below the surface.[77] Observation of these cracks became increasingly difficult after ~10–15 min. This effect is attributed to equilibration of the sample with ambient temperature, which resulted in melting of the ice wedging open the cracks.

Fig. 21. Samples used in comparative warping experiments, the results of which are shown in Fig. 19, clearly illustrate the difference in damage observed with (a) pure water, or (b) and (c) 3% NaCl. The thickness of the scaling damage is ~ 1–2 mm. The critical stress intensity for a crack propagating parallel to the interface at this depth is 0.1–0.25 $MPa \cdot m^{-0.5}$.

Fig. 22. Mortar samples after warping experiments with (a) and (c) 3% NaCl solution, or (b) pure water. (c) Scaling damage removed from the sample is finer than that yielded by the cement paste (Fig. 21). This is a direct result of the interfacial transition zone dominating the fracture process.
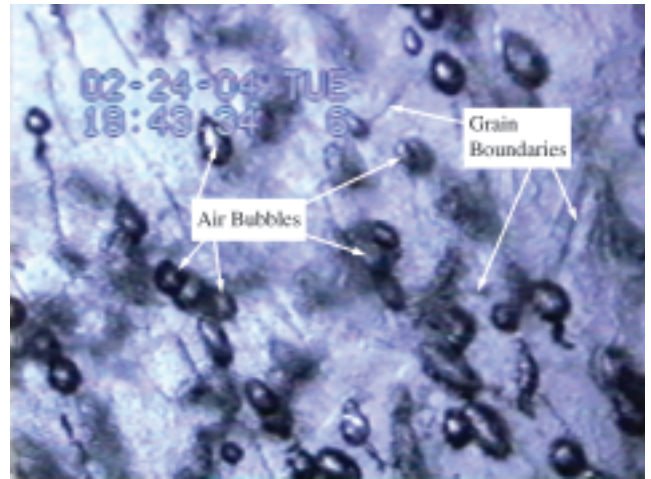

Fig. 23. Still photo taken from video of freezing experiment with pure water in a sandblasted glass cup. No cracking occurs in pure water ice, even though the temperature was rapidly reduced to $\sim -18^\circ C$. The imperfections in the ice are air bubbles, expelled upon solidification, and grain boundaries.

It is clear from Fig. 26 that there is no cracking in the area underneath the ice island. Furthermore, the bottom of the sample, which was also covered with vacuum grease, did not exhibit any cracking. To be absolutely certain that the cracks shown in Figs. 26 and 27 are a result of the glue-spall mechanism, similar experiments were performed where adjacent compartments were
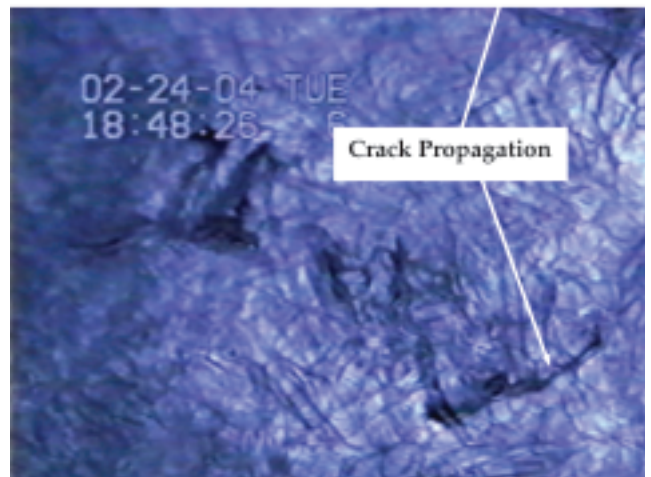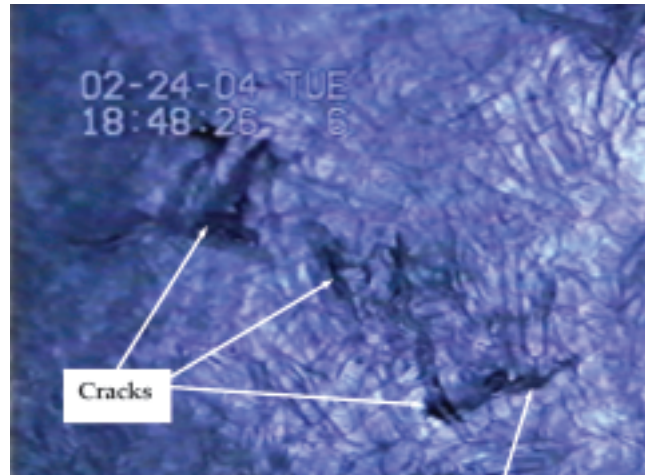

Fig. 24. Two still photos taken nearly 1 s apart from video of freezing experiment with a 3% sodium chloride solution. Comparison of the photos reveals crack propagation.
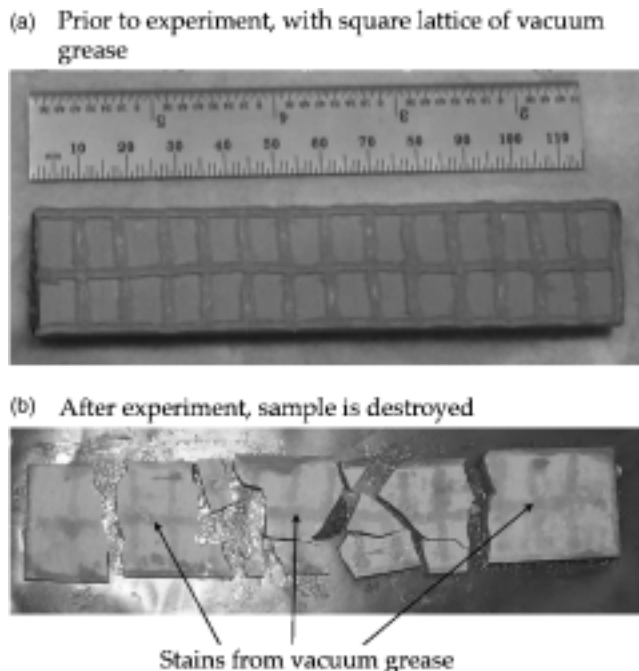
(a) Prior to experiment, with square lattice of vacuum grease

(b) After experiment, sample is destroyed

Stains from vacuum grease

Fig. 25. (a) Cement paste plate ($t_c = 5.04$ mm) with a square lattice of vacuum grease on the top surface. The square compartments are filled with pure water to a height of ~1–3 mm before the experiment. (b) Cement paste plate after warping experiment with pure water in 28 compartments, showing that the sample was destroyed by exposure to low temperature. The surface area stained by vacuum grease was investigated for surface cracking.

left dry. After exposure to a low temperature, the area under a vacuum grease partition between two adjacent dry compartments was compared with that under a partition adjacent to an ice island. No cracking was observed under the vacuum grease partition of two adjacent dry compartments, while cracking parallel to a wet compartment was clearly visible.

(3) Discussion and Conclusions

The results of the warping experiments indicate that salt changes the dominant mechanism active when a pool is frozen on the surface of a cement plate. When pure ice was compartmentalized on a borosilicate glass plate, it was observed that as the number of compartments increased (corresponding to a highly cracked ice layer), the amount of bi-material bending decreased. To verify that the frozen brine layer does crack, microscopy experiments were performed to investigate the behavior of various solutions upon solidification. It was observed that pure water did not fail upon cooling, while cracking was clearly visible when a 3% NaCl solution was cooled below $-10°$C. As expected, no cracking was observed when highly concentrated ($>7\%$–10%) solutions were frozen.

Once it was determined that an ice layer formed from a 3% NaCl solution is expected to fail, it was necessary to determine whether or not the corresponding ice islands would result in edge cracking from the glue-spall mechanism. To mimic failure, a pure ice layer was compartmentalized (Fig. 25) on the surface of a plate, and the area under the partitions was analyzed for the occurrence of glue-spall cracks. It was clearly shown that the ice islands cause edge cracks that circumscribe their perimeter (Fig. 26). Moreover, when two adjacent compartments were left dry, no cracking was observed under the common partition. When a pure ice layer was divided into 28 compartments (Fig. 25), the resulting composite exhibited concave down warping similar to that observed during low-temperature warping experiments with 3% NaCl solution (Fig. 19). This deflec-
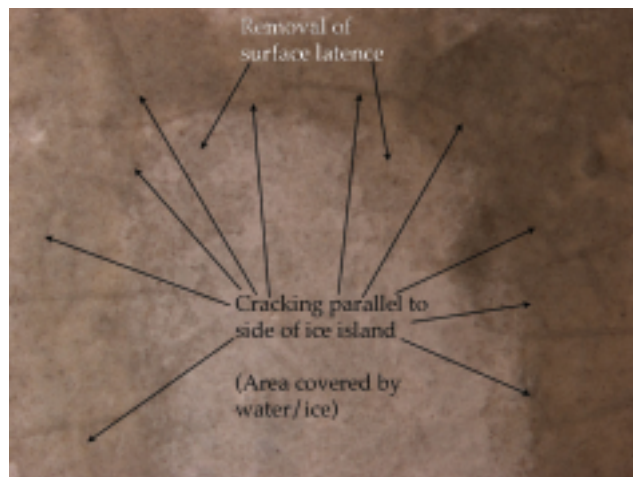

Fig. 26. Closeup of one of the compartments in Fig. 25 after warping experiment with compartmentalized water. The perimeter of the ice island corresponds to the areas stained by vacuum grease. The picture clearly indicates cracking along the perimeter of the island from the glue-spall mechanism. Also shown is removal of the surface laitance from the shear stress at the interface.

tion is attributed to ice wedging (see sidebar 5, Ice Wedging) in cracks created by glue-spalling.

The best evidence for the scaling mechanism is the difference in damage morphology shown in Figs. 21 and 25, corresponding to the 3% NaCl solution and compartmentalized water experiments, respectively. The latter picture shows that while the cracks are either parallel or perpendicular to the plate, all of the cracks run through the entire thickness of the plate. The direction of the cracks suggests that they were initiated by the glue-spall mechanism, because the vacuum grease partitions are all drawn either parallel or perpendicular to the edge of the plate. The fact that *all* of the cracks are through-cracks indicates that the mechanism that drives crack penetration clearly dominates the fracture process. In the case of pure ice, once the cracks are opened on the surface, the glue-spall stress has very little influence on the crack trajectory, because ice wedging becomes dominant. In contrast, the crack pattern observed with the 3% NaCl solution was random. This is consistent with the formation of cracks in the brine ice layer, which is dictated only by the location of brine pockets. Once the glue-spall cracks are opened, they follow a trajectory that turns parallel to the interface at a shallow depth. This indicates that the glue-spall stress is dominating the fracture process.

The different damage morphologies (Figs. 21 and 25) are attributed to the effect of salt on the ability of ice to wedge open surface cracks. With pure water, the entire pool on the surface is
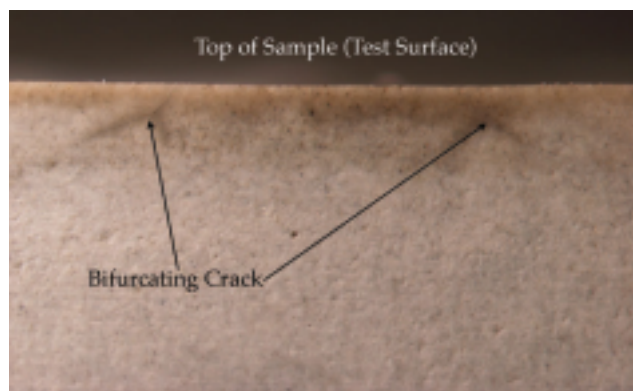

Fig. 27. Edge view of cracks that intersects the edge of the sample. In accord with the theory discussed in Section *VI*, the crack bifurcates under the surface.

frozen, so once the surface cracks are opened, the moisture necessary to fill the cracks with ice wedges is provided by the pore solution. As the temperature is further reduced the driving force for crack penetration increases. In the warping experiment with compartmentalized water, the large undercooling resulted in ice wedging dominating the fracture process, leading to the formation of numerous through-cracks.

In the experiment with 3% NaCl, once the glue-spall cracks are opened, they are filled with concentrated brine from brine pockets breached by fracture of the ice layer. As the temperature is further reduced, ice will form from this brine, but the stiffness of the wedges is reduced by the presence of brine pockets.[49] Furthermore, the stress that the brine imposes is much less than that realized with pure water ice, because the ice is in contact with a solution very close to its melting point. That is, the brine/ice is at a temperature that constitutes a small undercooling, which results in a small stress on the fracture surface. Therefore, in the warping experiment with 3% NaCl solution the glue-spall stress dominates the fracture process, while the small stress from ice wedging contributes to a concave down deflection. As the total deflection occurs over a period of 700 min (Fig. 19), the magnitude of the strain is affected by creep of the CM. In addition, the damage realized during this experiment represents a reduction in the effective thickness of the plate. If the material is removed progressively, then some of the deflection may also be attributed to a reduction in the stiffness of the substrate.

From the results presented above, we can conclude that a moderately concentrated ($\sim$3%) salt solution results in an ice layer that will crack when it forms a composite with a cementitious slab. A pure ice layer will not crack under the same conditions, and highly concentrated brine will result in ice that has no mechanical integrity in the temperature range of interest. The pessimum concentration arises, because it is necessary for the ice layer to fail to cause glue-spall damage in the substrate. When an ice layer fails, glue-spall cracking is expected to circumscribe the corresponding islands. It is necessary for the glue-spall mechanism to open surface cracks for ice wedging to occur, but when salt is present, it is not expected that ice wedging will dominate the fracture process. Combined with the analysis presented in Sections *III–VI*, the experimental results provide strong evidence for the primary importance of the glue-spall mechanism.

IX. Characteristics of Salt Scaling

Here, we summarize how the glue-spall mechanism accounts for the salt scaling characteristics outlined in Section *II*.

1. *Salt scaling consists of the progressive removal of small flakes or chips of binder*:
The morphology of damage from glue-spalling is similar to that observed from salt scaling. The damage should be progressive. The fracture mechanics analysis (Section *VII*) indicates that the depth of scalloping depends only on the mechanical properties and dimensions of the constituents. If the properties of the surface do not vary significantly with depth, then with each freeze/thaw cycle a relatively consistent amount of material will be removed by this mechanism. Once the coarse aggregate is exposed, the ice layer will bind to the surface of the aggregates, and cracks in the ice above aggregate will not result in damage, so the rate of removal of material per unit area in each freeze/thaw cycle should eventually drop off. Accordingly, when sawn surfaces are tested in scaling experiments, the scaling rate is very similar to that realized on a finished surface, if the weight loss is calculated based on the fraction of the surface occupied by cementitious binder.[96]

2. *A pessimum exists at a solute concentration of $\sim$3%, independent of the solute used*:
The glue-spall mechanism requires that the ice layer crack to result in scaling damage. The viscoelastic stress calculation (Section *V*) indicates that the pessimum concentration is a consequence of the effect of brine pockets on the mechanical

properties of ice: (i) because of creep, pure ice will not crack; (ii) the stress rises faster than the strength in ice formed from a moderately concentrated brine; and (iii) more highly concentrated solutions produce ice that has no strength in the temperature range of interest. The same behavior is observed with various solutes because the solutes exhibit similar melting point reductions as a function of solute concentration. Therefore, the microstructure of the brine ice is consistent, which suggests that the fracture and creep behavior are also consistent.

3. *No scaling occurs without a pool of liquid on the surface*:
There is no composite, and no stress, without the pool.

4. *No scaling occurs above $T = -10°C$*:
Ice formed from a 3% NaCl solution, which is used in all conventional tests, does not have strength above this temperature. *The severity of scaling damage increases as the minimum temperature is reduced*:
The glue-spall stress is proportional to the undercooling, ΔT (Eq. (3)), so smaller and smaller flaws will propagate as the temperature drops.

5. *Air entrainment reduces salt scaling damage*:
Air entrainment reduces bleeding,[54,55,97,98] so it produces a stronger surface. The beneficial effect of AEA is expected for all test surfaces (i.e., finished, molded, or sawn), because the effect on bleeding is realized throughout the concrete body. Furthermore, when an effective air-entraining agent is properly utilized, initial freezing in air voids imposes suction in the pore fluid that compresses the porous skeleton (sidebar 3, Internal Frost Action).[10,16,99]

6. *The salt concentration of the pool on the surface is more important than the salt concentration in the pore solution*:
The pore liquid has no effect on the severity of the glue-spall stress, because internal ice formation does not play a role in salt scaling.[16]

7. *Susceptibility to salt scaling is not correlated with susceptibility to internal frost action*:
The glue-spall mechanism is not related to internal crystallization.

8. *The strength of the surface governs the ability of a cementitious body to resist salt scaling*:
The strength of the finished surface is important, because the estimated glue-spall stress is marginal with respect to the tensile strength of the CM ($\sim$3 MPa). Any treatment or handling expected to weaken the surface (e.g., bleeding) will therefore result in more scaling.

X. Conclusions

Salt scaling contributes to exorbitant repair costs for the United States infrastructure. To prevent this damage, an understanding of the mechanism that results in salt scaling is necessary. In this paper, we have provided theoretical and experimental evidence demonstrating that the glue-spall mechanism accounts for all the characteristics of salt scaling.

An understanding of this mechanism indicates that salt scaling can be prevented by increasing the toughness of the surface, which is the weakest portion of a concrete body. It is clearly beneficial to prevent bleeding or handling that exacerbates the effects of bleeding.[17] Scaling might also be reduced by the inclusion of fibers, which hinder crack propagation.

References

[1]"Nonconventional Concrete Technologies: Renewal of the Highway Infrastructure," National Research Council, NMAB-484, National Academy Press, Washington, DC, 1997.

[2]H. Arnfelt, *Damage on Concrete Pavements by Wintertime Salt Treatment*, Meddelande 66 Statens Väginstitut, Stockholm, 1943.

[3]G. J. Verbeck and P. Klieger, "Studies of "Salt" Scaling of Concrete," *Highway Res. Board. Bull.*, **150**, 1–17 (1957).

[4]D. Jana, "Concrete Construction or Salt—Which Causes Scaling?," *Concr. Int.*, **26** [11] 31–8 (2004).

[5]C. Alonso, C. Andrade, M. Castellote, and P. Castro, "Chloride Threshold Values to Depassivate Reinforcing Bars Embedded in a Standardized OPC Mortar," *Cem. Concr. Res.*, **30**, 1047–55 (2000).

[6]W. G. Hime, "The Corrosion of Steel—Random Thoughts and Wishful Thinking," **15** [10] *Concr. Int.*, 54–7 (1993).

[7]D. Beckett, "Influence of Carbonation and Chlorides on Concrete Durability," *Concrete*, 16–8 (1983).

[8]G. Fagerlund, "The International Cooperative Test of the Critical Degree of Saturation Method of Assessing the Freeze/Thaw Resistance of Concrete," *Mater. Constr.*, **10** [58] 230–51 (1977).

[9]G. W. Scherer, "Crystalization in Pores," *Cem. Concr. Res.*, **29**, 1347–58 (1999).

[10]G. W. Scherer and J. J. Valenza, "Mechanisms of Frost Damage"; pp. 209–46 in *Materials Science of Concrete*, Vol. VII, Edited by J. Skalny, and F. Young. American Ceramic Society, Westerville, Ohio, 2005.

[11]S. Lindmark, "Mechanisms of Salt Frost Scaling of Portland Cement-Bound Materials: Studies and Hypothesis"; Ph.D. Thesis (Report TVBN 1017), Lund Institute of Technology, Lund, Sweden, 1998.

[12]E. J. Sellevold and T. Farstad, "Frost/Salt Testing of Concrete: Effect of Test Parameters and Concrete Moisture History," *Nordic Concr. Res.*, **10**, 121–38 (1991).

[13]P. E. Petersson, "The Influence of Silica Fume on the Salt Frost Resistance of Concrete"; Technical Report SP-RAPP 1986:32, Division of Building Technology, Swedish National Testing Institute, 1986.

[14]W. Studer, "Internal Comparative Tests on Frost-Deicing Salt Resistance"; pp. 175–87 in *International Workshop on the Resistance of Concrete to Scaling Due to Freezing in the Presence of Deicing Salts*. Centre de Recherche Interuniversitaire sur le Beton, Université de Sherbrooke - Université Laval, Quebec, August 1993.

[15]J. Marchand, M. Pigeon, D. Bager, and C. Talbot, "Influence of Chloride Solution Concentration of Salt Scaling Deterioration of Concrete," *ACI Mater. J.*, **96** [4] 429–35 (1999).

[16]J. J. Valenza II and G. W. Scherer, "A Review of Salt Scaling: II. Mechanisms"; *Cem. Concr. Res.*, (2006), submitted.

[17]J. J. Valenza II and G. W. Scherer, "A Review of Salt Scaling: I. Phenomenology"; *Cem. Concr. Res.*, (2006), submitted.

[18]ASTM "Standard Test Method for Scaling Resistance of Concrete Surfaces Exposed to Deicing Chemicals"; pp. 341–3 in *ASTM Standard C672. Annual Book of ASTM Standards*, Vol. 04.02, Edited by American Society for Testing and Materials, Philadelphia, 1992.

[19]SIS Concrete Testing—Hardened Concrete—Frost Resistance. Standardiserings-kommissionen i Sverige, Swedish Standard 13 72 44, 1992.

[20]M. J. Setzer, "On the Abnormal Freezing of Pore Water and Testing of Freeze-Thaw and Deicer Salt Resistance"; pp. 3–20 in *International Workshop on the Resistance of Concrete to Scaling Due to Freezing in the Presence of Deicing Salts*. Centre de Recherche Interuniversitaire sur le Beton, Université de Sherbrooke - Université Laval, Quebec, August 1993.

[21]M. Pigeon and R. Pleau, *Durability of Concrete in Cold Climates*. E & FN Spon, London, 1995.

[22]S. Jacobsen, "Scaling and Cracking in Unsealed Freeze/Thaw Testing of Portland Cement and Silica Fume Concretes"; Thesis Report 1995: 101, Norwegian Institute of Techology, Trondheim, 1995, p. 55.

[23]J. Marchand, R. Pleau, and R. Gagné, "Deterioration of Concrete Due to Freezing and Thawing"; pp. 283–354 in *Materials Science of Concrete IV*, Edited by J. Skalny, and S. Mindess. American Ceramic Society, Westerville, OH, 1995.

[24]T. A. Hammer and E. J. Sellevold, "Frost Resistance of High-Strength Concrete"; pp. 457–87 in ACI Special Publication SP-121: High-Strength Concrete: Second International Symposium, Edited by W. T. Hester. American Concrete Institute, Detroit, 1990.

[25]S. Jacobsen, "Scaling and Cracking in Unsealed Freeze/Thaw Testing of Portland Cement and Silica Fume Concretes"; Thesis Report 1995: 101, Norwegian Institute of Technology, Trondheim, 1995, pp. 177–95.

[26]D. Stark, "Effect of Length of Freezing Period on Durability of Concrete"; Portland Cement Association Research and Development Bulletin RD096T, 1989.

[27]M. J. Setzer, "On the Abnormal Freezing of Pore Water and Testing of Freeze/Thaw and Deicing Salt Resistance"; pp. 3–17 in *International Workshop on the Resistance of Concrete to Scaling Due to Freezing in the Presence of Deicing Salts*. Centre de Recherche Interuniversitaire sur le Beton, Université de Sherbrooke - Université Laval, Quebec, August 1993.

[28]S. Jacobsen, T. Farstad, H. C. Gran, and E. J. Sellevold, "Frost Salt Scaling of No Slump Concrete: Effect of Strength," *Nordic Concr. Res.*, **11**, 57–71 (1991).

[29]P. C. Aitcin and M. Pigeon, "Performance of Condensed Silica Fume Concrete Used in Pavements and Sidewalks," *Durab. Build. Mater.*, **3**, 353–68 (1986).

[30]T. C. Powers, "A Working Hypothesis for Further Studies of Frost Resistance of Concrete," *J. Am. Concr. Inst.*, **16** [4] 245–72.

[31]J. Marchand, R. Gagné, S. Jacobsen, E. J. Sellevold, and M. Pigeon, "The Frost Durability of High-Performance Concrete," pp. 273–88 in *Concrete Under Servere Conditions: Environment and Loading*, *Vol. 1*, Edited by K. Sakai, N. Banthia, and O. E. Gjørv. E & FN Spon, 1995.

[32]G. W. Scherer, "Stress from Crystallization of Salt," *Cem. Concr. Res.*, **34**, 1613–24 (2004).

[33]A. Rösli and A. B. Harnik, "Improving the Durability of Concrete to Freezing and Deicing Salts"; pp. 464–73 in *Durability of Building Materials and Components*, ASTM Special Technical Publication STP-691, Edited by P. J. Sereda, and G. G. Litvan. ASTM, Philadelphia, 1980.

[34]O. Copuroglu, E. Schlangen, K. van Breugel, and A. L. A. Fraaij, "Frost Salt Scaling Modeling of Cement Paste"; *International Conference on Concrete Repair, Rehabilitation and Retrofitting*, ICCRRR 2005, Cape Town, South Africa.

[35]F. T. Wall, *Chemical Thermodynamics*. Freeman, San Francisco, 1965.

[36]G. W. Scherer, "Characterization of Saturated Porous Bodies," *Concr. Sci. Eng.*, **37** [265] 21–30 (2004).

[37]J. J. Valenza and G. W. Scherer, "Measuring the Permeability of Rigid Materials by a Beam-Bending Method: V. Isotropic Rectangular Plates of Cement Paste," *J. Am. Ceram. Soc.*, **87** [10] 1927–31 (2004).

[38]T. C. Powers, "The Air Requirement of Frost-Resistant Concrete," *Proc. Highway Res. Board*, **29**, 184–211 (1949).

[39]T. C. Powers and R. A. Helmuth, "Theory of Volume Changes in Hardened Portland-Cement Paste During Freezing," *Proc. Highway Res. Board*, **32**, 285–97 (1953).

[40]P. Klieger and S. Gebler, "Fly Ash and Concrete Durability"; pp. 1043–69 in ACI Special Publication SP-100: Concrete Durability: Proceedings of the Catherine and Brian Mather International Symposium, Edited by J. Scanlon. American Concrete Institute, Detroit, 1987.

[41]M. Pigeon, D. Perraton, and R. Pleau, "Scaling Test of Silica Fume Concrete and the Critical Spacing Factor Concept"; pp. 1155–82 in ACI Special Publication SP-100: Concrete Durability: Proceedings of the Catherine and Brian Mather International Symposium, Edited by J. Scanlon. American Concrete Institute, Detroit, 1987.

[42]C. Johnston, "Effects of Microsilica and Class C Fly Ash on Resistance of Concrete to Rapid Freezing and Thawing, and Scaling in the Presence of Deicing Agents"; pp. 1183–204 in ACI Special Publication SP-100: Concrete Durability: Proceedings of the Catherine and Brian Mather International Symposium, Edited by J. Scanlon. American Concrete Institute, Detroit, 1987.

[43]S. H. Gebler and P. Klieger, "Effect of Fly Ash on the Durability of Air-Entrained Concrete"; pp. 483–519 in ACI Special Publication SP-91: Fly Ash, Silica Fume, Slag, and Natural Pozzolans in Concrete, Edited by V. M. Malhotra. American Concrete Institute, Detroit, 1986.

[44]C. Foy, M. Pigeon, and N. Banthia, "Freeze-Thaw Durability and Deicer Salt Scaling Resistance of a 0.25 Water–Cement Ratio Concrete," *Cem. Concr. Res.*, **18**, 604–14 (1988).

[45]R. E. Beddoe and M. J. Setzer, "A Low Temperature DSC Investigation of Hardened Cement Paste Subjected to Chloride Action," *Cem. Concr. Res.*, **18**, 249–56 (1988).

[46]S. T. Gulati and H. E. Hagy, "Analysis and Measurement of Glue-Spall Stresses in Glass–Epoxy Bonds," *J. Am. Ceram. Soc.*, **65** [1] 1–5 (1982).

[47]S. T. Gulati and H. E. Hagy, "Theory of the Narrow Sandwich Seal," *J. Am. Ceram. Soc.*, **61** [5–6] 260–3 (1973).

[48]E. R. Pounder, *Physics of Ice*. Pergamon Press, Oxford, 1965.

[49]R. E. Gagnon and S. J. Jones, "Elastic Properties of Ice"; pp. 229–57 in *Handbook of Elastic Properties of Solids, Liquids, and Gases, Vol. III: Elastic Properties of Solids: Biological and Organic Materials (Chapter 9)*, Edited by M. Levy, H. Bass, and R. Stern. Academic Press, New York, 2001.

[50]J. P. Ciardullo, D. J. Sweeney, and G. W. Scherer, "Thermal Expansion Kinetics: Method to Measure the Permeability of Cementitious Materials: IV, Effect of Thermal Gradients," *J. Am. Ceram. Soc.*, **88** [5] 1213–21 (2005).

[51]J. J. Valenza II, "Mechanism for Salt Scaling"; Ph. D. Thesis, Princeton University, 2005. www.jvalenza.com/thesis.html.

[52]K. L. Scrivener, A. K. Crumbie, and P. Laugesen, "The Interfacial Transition Zone (ITZ) Between Cement Paste and Aggregate in Concrete," *Interf. Sci.*, **12**, 411–21 (2004).

[53]K. L. Scrivener, A. Bentur, and P. L. Pratt, "Quantitative Characterization of the Transition Zone in High Strength Concretes," *Adv. Cem. Res.*, **1** [4] 230–7 (1988).

[54]A. M. Neville, *Properties of Concrete*. John Wiley and Sons, Inc., New York, NY, 1996.

[55]S. Mindess and F. Young, *Concrete*, pp. 353–62. Prentice-Hall, Inc., Englewood Cliffs, NJ, 1981.

[56]D. A. Porter and K. E. Easterling, *Phase Transformations in Metals and Alloys*, 2nd edition, Stanley Thornes, Cheltenham, UK, 1992.

[57]J. Weissenberger, G. Dieckmann, R. Gradinger, and M. Spindler, "Sea Ice: A Cast Technique to Examine and Analyze Brine Pockets and Channel Structure," *Limnol. Oceanogr.*, **37** [1] 179–83 (1992).

[58]H. Eicken, C. Bock, R. Wittig, H. Miller, and H. O. Poertner, "Magnetic Resonance Imaging of Sea Ice Pore Fluids: Methods and Thermal Evolution of Pore Microstructure," *Cold Reg. Sci. Tech.*, **31**, 207–25 (2000).

[59]W. F. Weeks, "Tensile Strength of NaCl Ice," *J. Glaciol.*, **4**, 25–52 (1962).

[60]Z. Hashin and S. Shtrikman, "A Variational Approach to the Theory of the Elastic Behavior of Multiphase Materials," *J. Mech. Phys. Solids*, **11**, 127–40 (1963).

[61]S. Torquato, *Random Heterogeneous Materials: Microstructure and Macroscopic Properties*. Springer-Verlag, New York, 2001.

[62]G. W. Scherer and J. J. Valenza, "Mechanism for Salt Scaling of a Cementitious Surface," *Concr. Sci. Eng.*, 2005, in press.

[63]W. Weeks and A. Assur, "The Mechanical Properties of Sea Ice. Part II: Physical Science. Section C: Physics and Mechanics of Ice"; Cold Regions Research and Engineering Lab, Hanover, NH. DA Project 1VO25001A130.

[64]P. Barnes, D. Tabor, and J. C. F. Walker, "The Friction and Creep of Polycrystalline Ice," *Proc. R. Soc. London Ser. A*, **324** [1557] 127–55 (1971).

[65]G. W. Scherer, "Editorial Comments on a Paper by Gordon S. Fulcher," *J. Am Ceram. Soc.*, **75** [5] 1060–2 (1992).

[66]R. C. Weast, and M. J. Astle eds., *CRC Handbook of Chemistry and Physics*, 77th edition, CRC Press, Boca Raton, FL, 1996 pp. 6–139.

[67]L. E. Raray and D. Tabor, "The Adhesion and Strength Properties of Ice," *Proc. R. Soc. London A*, **245** [1241] 184–201 (1958).

[68]S. P. Shah, S. E. Swartz, and C. Ouyang, *Fracture Mechanics of Concrete*. John Wiley & Sons, 1995.

[69]T. Ye, Z. Suo, and T. Evans, "Thin Film Cracking and the Roles of Substrate and Interface," *Int. J. Solid Struct.*, **29**, 2639–48 (1992).

[70]A. B. Abell and D. A. Lange, "The Role of Crack Deflection in Toughening of Cement-Based Material"; pp. 241–50 in *International Symposium on Proceedings of Brittle Matrix Composites 5*, Edited by A. M. Brandt, V. C. Li, and L. H. Marshall. BIGRAF, Warsaw, 1997.

[71]L. Zhang and F. P. Glasser, "Critical Examination of Drying Damage to Cement Pastes," *Adv. Cem. Res.*, **12** [2] 79–88 (2000).

[72]C. Galle, "Effect of Drying on Cement-Based Materials Pore Structure as Identified by Mercury Intrusion Porosimetry. A Comparative Study Between Oven-, Vacuum-, and Freeze-Drying," *Cem. Concr. Res.*, **31**, 1467–77 (2001).

[73]C.-L. Hwang and J. F. Young, "Drying Shrinkage of Portland Cement Pastes I. Microcracking During Drying," *Cem. Concr. Res.*, **14**, 585–94 (1984).

[74]J. Bisschop and J. G. M. van Mier, "How to Study Drying Shrinkage Microcracking in Cement-Based Materials Using Optical and Scanning Electron Microscopy," *Cem. Concr. Res.*, **32**, 279–87 (2002).

[75]M. D. Thouless, A. G. Evans, M. F. Ashby, and J. W. Hutchinson, "The Edge Cracking and Spalling of Brittle Plates," *Acta Metall.*, **35** [6] 1333–41 (1987).

[76]M. D. Drory, M. D. Thouless, and A. G. Evans, "On the Decohesion of Residually Stressed Thin Films," *Acta. Metall.*, **36** [8] 2019–28 (1998).

[77]M. D. Drory and A. G. Evans, "Experimental Observations of Substrate Fracture Caused by Residually Stressed Films," *J. Am. Ceram. Soc.*, **73** [3] 634–8 (1990).

[78]H. Tada, P. C. Paris, and G. R. Irwin, *The Stress Analysis of Cracks Handbook*, p. 2.25. Del Research Corp., St. Louis, MO, 1985.

[79]S. Timoshenko, "Analysis of Bi-Metal Thermostats," *J. Opt. Soc. Am.*, **11**, 233–55 (1925).

[80]G. W. Scherer, *Relaxation in Glasses and Composites*. Wiley, New York, 1986.

[81]J. Marchand, B. Gerard, and A. Delgrave, "Ion Transport Mechanisms in Cement-Based Materials"; pp. 307–99 in *Materials Science of Concrete*, **Vol. V**, Edited by J. Skalny, and S. Mindess. American Ceramic Society, Westerville, OH, 1998.

[82]J. Stark and S. Stürmer, "Investigation of Compatibility of Cements with Several Salts"; paper 4-iv-031 in *Proceedings of the 10th International Congress on the Chemistry of Cement*, Vol. 4 SINTEF, Trondheim, Norway, 1997

[83]S. Y. Hong and F. P. Glasser, "Alkali Binding in Cement Pastes. Part I. The C–S–H Phase," *Cem. Concr. Res.*, **29**, 1893–903 (1999).

[84]H. Viallis, P. Faucon, J. C. Petit, and A. Nonat, "Interaction between Salts (NaCl, CsCl) and Calcium Silicate Hydrates (C–S–H)," *J. Phys. Chem. B*, **103**, 5212–9 (1999).

[85]U. Wiens and P. Schiessl, "Chloride Binding of Cement Paste Containing Fly Ash"; paper 4-iv-016 in *Proceedings of the 10th International Congress on the Chemistry of Cement*, Vol. 4. SINTEF, Trondheim, Norway, 1997

[86]U. A. Birnin-Yauri and F. P. Glasser, "Friedel's Salt, $Ca_2Al(OH)_6$ $(Cl,OH) \cdot 2H_2O$: Its Solid Solutions and Their Role in Chloride Binding," *Cem. Concr. Res.*, **28** [12] 1713–23 (1998).

[87]A. K. Suryavanshi, J. D. Scantlebury, and S. B. Lyon, "Mechanism of Friedel's Salt Formation in Cements Rich in Tri-Calcium Aluminate," *Cem. Concr. Res.*, **26** [5] 717–27 (1996).

[88]J. J. Valenza and G. W. Scherer, "Mechanisms of Salt Scaling," *Mater. Struct.*, **38**, 479–88 (2005).

[89]J. J. Valenza II, S. Vitousek, and G. W. Scherer, "Expansion of Hardened Cement Paste in Saline Solutions"; pp. 207–12 in *Creep, Shrinkage and Durability of Concrete Structures*, Edited by G. Pijaudier-Cabot, B. Gérard, and P. Acker. Hermes, London, 2005

[90]J. J. Völkl, R. E. Beddoe, and M. J. Setzer, "The Specific Surface of Hardened Cement Paste by Small Angle X-Ray Scattering Effect of Moisture Content and Chlorides," *Cem. Concr. Res.*, **17**, 81–8 (1987).

[91]R. C. Weast, and M. J. Astle eds., *CRC Handbook of Chemistry and Physics*, 77th edition, CRC Press, Boca Raton, FL, 1996 pp. 8–73.

[92]F. T. Wall, *Chemical Thermodynamics*. Freeman, San Francisco, 1965 pp. 157–8.

[93]H. Tada, P. C. Paris, and G. R. Irwin, *The Stress Analysis of Cracks Handbook*. Del Research Corp., St. Louis, MO, 1985 p. 194.

[94]J. J. Valenza II and G. W. Scherer, "Evidence of Anomalous Thermal Expansion of Water in Cement Paste," *Cem. Concr. Res.*, **35**, 57–66 (2005).

[95]W. Vichit-Vadakan and G. W. Scherer, "Measuring Permeability of Rigid Materials by a Beam-Bending Method: III. Cement Paste," *J. Am. Ceram. Soc.*, **85** [6] 1537–44 (2002).

[96]J. Marchand, M. Pigeon, J. Boisvert, H. L. Isabelle, and O. Houdusse, "Deicer Salt Scaling Resistance of Roller Compacted Concrete Pavements Containing Fly Ash and Silica Fume"; pp. 151–78 in ACI Special Publication SP-132: Fly Ash, Silica Fume, Slag, and Natural Pozzolans in Concrete — Proceedings Fourth International Conference, Istanbul, Turkey, May 1992. Edited by V.M. Malhotra. American Concrete Institute, Detroit, 1992.

[97]G. M. Bruere, "Mechanisms by which Air-Entraining Agents Affect Viscosities and Bleeding Properties of Cement Pastes," *Austral. J. Appl. Sci.*, **9**, 349–59 (1958).

[98]T. C. Powers, *The Properties of Fresh Concrete*. John Wiley and Sons, Inc., New York, 1968.

[99]G. W. Scherer, J. Chen, and J. Valenza, "Method of Protecting Concrete from Freeze/Damage"; U.S. Patent 6 485 560, November 26, 2002.   □

George W. Scherer received his B.S. and M.S. degrees in 1972 and his PhD in materials science in 1974, all from MIT. From 1974 to 1985, he was at Corning Glass Works, where his research included optical fiber fabrication, viscous sintering, and viscoelastic stress analysis. From 1985 through 1995, he was a member of the Central Research Department of the DuPont Company, where his work dealt principally with sol–gel processing, and especially with drying. In February, 1996, he became a full professor in the Department of Civil & Environmental Engineering at Princeton University, and a member of the Princeton Institute for the Science & Technology of Materials.

He has received the Morey (1985), Purdy (1986), Fulrath Pacific (1990), Sosman (1994), and Brunauer (2001 and 2002) Awards from the ACerS, and the Iler Award from the American Chemical Society (1995). In 1997 he was elected to the National Academy of Engineering. He is the author of two books, ~200 papers, and 10 US patents.

John Valenza earned his BS in 1999 in civil engineering, from Virginia Tech, and his Ph.D. in materials science in 2005, from Princeton. His graduate work was focused on poromechanics, the structure and properties of confined fluids, and durability issues that face porous media. He has contributed to 10 papers and 1 US patent. The objective of his thesis was to identify the mechanism responsible for salt scaling.

He is a member of the Virginia Tech honors society, and has received an NSF REU grant (1998), and a graduate fellowship from the Princeton Materials Institute (2000–2005). In addition, he has performed independent research in the laboratories of George W. Scherer (1999), and W.R. Grace and Co. Cambridge, MA (2000). He is a member of the American Ceramic Society, the Materials Research Society, and the American Society of Civil Engineers. Currently, he is a post-doctoral research associate at the Princeton Institute for the Science and Technology of Materials, in association with the Department of Civil Engineering at Princeton University. His research is focused on deterioration of stone by salt crystallization, and the thermodynamics of crystallization pressure.